ORIGINAL ARTICLE

Performance based probabilistic seismic risk assessment for urban heritage. An example in *Pla del Remei Area* (Valencia)

Arianna Guardiola-Víllora[1] · Sergio Molina[2,3] · Dina D'Ayala[4]

© The Author(s) 2023

Abstract

The assessment of the seismic behaviour of historic residential buildings and the estimation of their possible losses in the event of an earthquake, is a must for defining strategic mitigation plans to prevent irreplaceable heritage losses. In this study an integrated performance based probabilistic risk assessment methodology is developed. An archival study and a field survey allow to identify architectural and construction characteristics of heritage residential buildings in urban areas and determine realistic structural models. These are analysed by using a limit state approach, coded in the FaMIVE method, considering different construction hypotheses, to produce capacity curves which support the identification of a discrete number of typologies representative of the entire building stock in the area. Their fragility functions are then derived using the modified N2 method. Because of the difficulty in quantifying the expected probable losses in purely economic terms, given the heritage value of these assets, losses are computed in terms of damaged floor surface area and mean damage ratio. These have been obtained through the earthquake loss estimation platform SELENA, considering different possible seismic scenarios. The procedure is applied to masonry residential buildings in *Pla del Remei* area of Valencia, Spain, built between the end of the 19th Century and the end of the Spanish War (1939). This neighbourhood embodies the cultural values, construction techniques and historic legacy of a new and brief era of modernity, inspired by the new urban theories and architectural styles of Eclecticism and Modernism. Despite Valencia being located in an area of low to moderate seismicity, the results show that the maximum percentage of built damaged area ranges from 5.8 to 11.6% for 475 years return period, increasing to 33.59–51.59% for 975 years return period. The high level of resolution of the study allows mapping and identifying the structures at higher risk and is therefore a valuable tool to support sensitive and targeted retrofitting policies.

Keywords Heritage losses in Residential Masonry Buildings · *Pla del Remei* (Valencia) · FaMIVE · SELENA

Extended author information available on the last page of the article

1 Introduction

Several approaches are available in literature to assess the seismic vulnerability of buildings and estimate their physical, economic and social losses at urban scale (Erdik and Dukural 2006, Carreño et al. 2007; Liu et al. 2019). The Project Global Earthquake Model (GEM) provide guidance on selection of suitable numerical methods depending on the scale and objectives of the study, data availability and quality, and the expected results (D'Ayala et al. 2015). A recent comprehensive review of methods for the seismic vulnerability and risk assessment for masonry buildings has been compiled by Shabani et al. (2021). Many of these methods are coded within GIS-based platforms which allow to integrate data on hazard, exposure and vulnerability, and to visualize risk in geographic terms: HAZUS- MH (FEMA 2003, 2020), Openquake (Pagani et al. 2014); SELENA (Molina et al. 2010); CAPRA (Cardona et al. 2012); Armagedom (Sedan et al. 2013), amongst others.

For historic city centres, the empirical vulnerability approach is commonly used. This consists on quantifying a Vulnerability Index based on the scoring and weighting of a number of parameters that are considered to be influential in determining the damageability of given building types when exposed to seismic action. This approach, originally developed by Benedetti et al. (1988), has seen several adaptations and applications to diverse urban fabrics and masonry typologies (Lagomarsino and Giovinazzi (2006), Feriche et al. (2009), Lantada et al. (2010), Irizarri et al. (2011), Irizarry et al. (2012), Feriche (2012), Martínez-Cuevas and Gaspar-Escribano (2016), Ferreira et al. (2017), Lantanda et al. (2018), Guardiola-Víllora and Basset-Salom (2020), Vetore et al. (2020)).

The method has the advantage of producing fragility functions correlating a macro seismic intensity measure to a mean damage ratio, using either binomial or logarithmic distributions. Nonetheless each application needs calibration, which is difficult to achieve in absence of pre-existing seismic damage surveys, depends largely on expert opinion, on local geomorphology, seismology and assets distribution.

Analytical vulnerability assessment methods have greater data and computational requirements; however, they are also more versatile in their applicability. Methods suitable for assessment of large number of buildings described by a relatively small number of parameters, necessarily rely on relatively simple structural approaches, for instance collapse mechanism-based methods (Bernardini et al. 1990; D'Ayala and Speranza 2003, Donà et al. 2021), capacity spectrum-based methods (Fajfar 1999; FEMA 2003; Irizarry et al. 2011), or displacement-based methods (Ahmad et al. 2010). The first of these methods relies on simplifying the structure in large subcomponents for which mechanisms can be identified and collapse load factors computed, representing the ultimate lateral strength capacity of the structure. The other two methods use simplified mechanical models to derive capacity curves on the basis of which both elastic and ultimate strength and displacement thresholds can be identified and compared with a linear or non-linear seismic demand spectrum, to determine performance and damage states (D'Ayala et al. 2015). When applied to large sets of buildings and/or considering a large number of alternative seismic spectra the computed results can be treated statistically to derive fragility and vulnerability functions, and can be then used to determine seismic risk, when combined with hazard and exposure (D'Ayala et al. 2015).

From a global perspective, Spain is located in an area of low to moderate seismic hazard (Pagani et al. 2020) Nonetheless, the earthquake that hit Lorca a decade ago (11 May 2011), caused serious damage to most of the town's cultural heritage, bringing to light that, in Spain, the risk of loss of architectural heritage due to seismic events is non-negligible.

Ruiz-Pinilla et al. (2016) pointed out that although the recorded Mw = 5.1 and max MMI = VI, classify this event as a moderate earthquake, the vicinity of the epicentre to the town, the directivity of the ground motion and the specific characteristics of the building stock in the regions were responsible for the severity, extent and variety of structural damage. More recently, Kharazian et al. (2021) have shown how, if the focus is shifted from uniform hazard based design, to targeted risk based design, current seismic demands in terms of peak ground acceleration might need updating to obtain uniform risk probability of exceedance for set limit states with specific return periods across the Spanish territory, also considering the effects related to specific structural typologies or construction features. While the concepts of maximum credible earthquake and targeted collapse probability have been used in design for a decade (ASCE 7–16 2018; Luco 2006), their application to existing historic buildings is not common. Conversely, the issue of targeted seismic risk assessment is particularly of relevance for typologies which are not seismically designed according to the code and for which therefore higher vulnerability and/or greater losses shall be expected.

Historic and minor heritage buildings in urban centres fall within this category, however, following the Lorca earthquake, 2010, it emerged that neither the basic guidelines for the generation of Special Plans nor the Heritage Plans (Ley 16/1985 del Patrimonio Histórico Español 1985) contained any recommendations addressing specific seismic risk and disaster management issues. As a consequence, in 2015, the Spanish Institute of Cultural Heritage (IPCE) of the Ministry of Education Culture and Sport (MECD) approved the National Emergency and Risk Management Plan for Cultural Heritage (Ministerio de Educación Cultura y Deporte 2015). One of the stated objectives is to analyse the degree of damage that Assets of cultural interest would suffer due to their location and characteristics, so that appropriate prevention of the consequences of natural hazards can be determined. The present methodology aims to respond to the demand for such tools.

In devising a targeted seismic risk assessment approach, the intensity and time horizon of the hazard is of primary concern. Spanish cultural heritage is classified in the Spanish Seismic Code -NCSE-02- (Ministerio de fomento 2002) as buildings of "special importance" (Ministerio de Fomento 2002) and additionally also Eurocode 8 (EN 1998-1 2004, CEN 2004) classifies them as "essential structures" (or class IV). Such classification would justify the choice of a seismic hazard corresponding to 975-year return period when evaluating the seismic risk posed to heritage buildings. The Italian seismic code NTC 2018, (MIT 2018) provides indications of different return periods for different damage thresholds in reference to the expected remaining life of the structure (Torelli et al. 2020) so that, assuming the residual life of these buildings is 50 years and no particular protection is considered, return periods of 475 years and 975 years should be considered for the life safety limit state and for the collapse prevention limit state, respectively. Indeed, Arto et al. (2020) carried out a vulnerability analysis of medieval rammed earth fortifications in south-eastern Spain computing the mean damage level taking into account a probabilistic scenario for a 975 year return period. On the other hand, Guardiola-Villora and Basset-Salom (2020) performed a seismic risk analysis of the residential buildings in the Ciutat Vella District of Valencia, the most important cultural heritage of the Valencian Community, (Govern Valencià 1993) using a deterministic and two probabilistic seismic scenarios corresponding to a 475-year return period. The issue of the appropriate level of hazards to be chosen in seismic risk assessment of historic centres remains an open question, as the codes do not explicitly categorise them.

The present study proposes an integrated methodology which includes the following tasks: (i) archival and on site research to identify and classify the assets at risk, including

definition of their architectural and heritage value to determine the detailed exposed portfolio in a city centre; (ii) site survey and analytical seismic vulnerability assessment to identify specific and recurring seismic responses and determine typologies and classification within the exposed building stock; (iii) disaggregation of the seismic hazard to define relevant seismic scenarios (probable and maximum) and (iv) compute the corresponding losses. Such assessment is an essential first step towards the proposal of prevention and mitigation measures compatible with the cultural and architectural heritage value of historic urban centres. The approach is applied to *Pla del Remei,* one of the wealthiest neighbourhoods in Valencia, Spain, where most of the Valencian Modernist heritage is located, representing the historic legacy and hallmark of the Valencian inhabitants. These buildings were designed to withstand only gravity loading, therefore the objective is to determine their seismic risk to support decision-making in terms of minimal necessary retrofitting.

To fulfil the first task, the buildings original drawings, available at the Municipal Historic Archive of Valencia (AHMV), were consulted to assess dimensions, construction and structural system. This was integrated with extensive on-site surveys, to understand their variability, and therefore evaluate the uncertainties in defining the structural models. This information is integrated with the Valencia Cadastral Database (SEC 2021) and mapped using the gvSIG mapping tool (gvSIG association 2009), to establish a permanent database of the exposure of this neighbourhood.

Considering the size of the sample and that the level of detail needed for a full material and structural characterisation is not available, a nonlinear dynamic analysis of each buildings is neither possible, nor viable. Instead, the Failure Mechanisms Identification and Vulnerability Evaluation method (FaMIVE, D'Ayala and Speranza 2003), is selected to deliver the second task above. This is a collapse mechanism-based procedure developed for vulnerability assessment of historic urban centres, that allows to adapt the routines to the specific construction characteristics of the building stock being analysed. All possible in-plane and out-of-plane collapse mechanisms are considered and therefore the failure mode is not pre-imposed on the structure, but it results from its specific characteristics. The FaMIVE method has been extended (D'Ayala 2013) to cover the steps of capacity spectrum-based methods, to produce capacity curves based on ultimate lateral strength capacity and elastic and ultimate displacement, and the corresponding fragility functions, in line with the N2 procedure (Fajfar and Dolsek 2012) also recommended in Eurocode 8 (EN 1998-1 2004, CEN 2004). FaMIVE has been used to correlate observed damage to collapse mechanisms and lateral capacity in L'Aquila, Italy, (D'Ayala and Paganoni 2011), and Lorca, Spain, (Basset-Salom and Guardiola-Víllora 2014) to define strength and displacement performance improvement due to interventions in Algiers, Algeria (Novelli et al. 2015), and study the effect of repeated main shocks in Norcia, Italy, following the Central Italy 2016 earthquake (Putrino and D'Ayala 2019).

The FaMIVE procedure allows the retention of a high level of detail of the geometry and kinematics for each building's façade, while minimizing computational and time demands, since it computes only the ultimate condition, without undertaking a full pushover analysis. Epistemic uncertainties concerning the reliability of input data from the on-site survey are contemplated by considering all numerical values in input with a margin of error dependent on the data acquisition procedure used. Uncertainties related to the derivation of the capacity curves, including damage thresholds, are accounted for, by performing extensive sensitivity analysis for the relevant parameters.

The definition of the relevant hazard scenarios and the risk analysis are performed with the earthquake loss estimation tool SELENA (Molina and Lindholm 2010), successfully applied to a multitude of testbeds worldwide, e.g. Oslo (Molina and Lindholm 2005),

Naples (Lang et al. 2008), Bucharest (Lang et al. 2012) the Romanian-Bulgarian border region (Erduran et al. 2012), among others, and more recently in the south and south-east of Spain, Adra (Molina et al. 2018) and Murcia (Molina et al. 2020). Coded in Matlab©, the main advantage of SELENA is the flexibility that the user has to configure the input data depending on the desired outcomes. Moreover, SELENA loss assessment is also based on the N2 method, and therefore seamlessly integrated with the FaMIVE procedure.

Section 2 presents a description of *Pla del Remei* historic urban development and current layout, providing the motivation for its choice as a case study. This information is essential to identify the relevant archival and cadastral sources, select the buildings to be included in the inventory and the specific elements and parameters to be considered in the design and development of the database, to fully characterise the exposure. The methodology used to conduct the seismic risk assessment is outlined in Sect. 3. The integrated database is described in Sect. 3.1 and the building inventory analysed to select a sample of the building stock to be used to characterise the vulnerability of *Pla del Remei* historic urban stock. The iterative use of FaMIVE to determine a reduced number of typologies with unique characteristic and correlated seismic performance is presented in Sect. 3.2; the determination of capacity curves and fragility functions for input in SELENA is then conducted using the N2 method. Section 3.3 is dedicated to the characterisation of the hazard, definition of the seismic scenarios in line with the SELENA procedure and the characterisation of the unit of assessment. Finally, results are spatially mapped in Sect. 4 in terms of the range of possible damage for each of the typologies, the mean damage ratio associated to each scenario, and a discussion on the impact of heritage value on the computed economic losses.

2 Description of *Pla del Remei* quarter

In probabilistic seismic risk assessment of historic urban centre, a realistic and accurate description of the building stock, constituting the exposure component of risk, is an essential ingredient, and one necessarily tied to the particular location chosen. For this study *Pla del Remei* quarter, in Valencia (Spain), part of the Artistic Historical Site of Valencia Historic Centre, declared Asset of Cultural Interest in 1993 (Govern Valencià 1993), is chosen, to demonstrate the need for accurate observation of the assets and the scale at which such investigation shall be conducted.

Pla del Remei quarter (in red in Fig. 1a) is the result of the extension of the old city centre of Valencia after the demolition of the mediaeval walls in 1865. The urban plan, known

Fig. 1 a. *Pla del Remei* quarter. b. 1884 Valencia's map (Llopis and Perdigón 2016)

Fig. 2 Building typologies in *Pla del Remei* quarter **a**, **b** Wealthy town houses. **c**, **d** Blocks of flats for rental. (*Source*: Authors 2021)

as the 1884 Eixample, finally approved in 1887 (Special Protection plan P.E.P 1, Ajuntament de València 2005), was designed to develop an area adjacent to the then city centre following the squared grid approach introduced by Ildefonso Cerdá for the expansion of the city of Barcelona (Colomer and García 1984). One of the main features of such design is the presence of wide chamfers in the corners of the resulting blocks that characterises the urban scene and determines the way in which the buildings are arranged in each block. In the case of *Pla del Remei*, the urban plan was adapted to the footprint of the demolished city walls, resulting in irregular blocks of irregular shape and size, defining the transition between the mediaeval and the modern urban layout.

At the end of the XIX century, the city of Valencia experienced a relative economic boom, mainly due to the export of agricultural products, but also the initial development of an industrial infrastructure (Taberner 1984). When the urban development of *Pla del Remei* was launched in 1884 (Fig. 1b) the Valencian bourgeoisie started to settle in this new quarter (Taberner and Broseta 2014). According to Daniel Benito Goerlich (Benito 1992a) two different aspects can be considered to catalogue the residential buildings of this area: the residential typology and the architectural style.

From the point of view of the residential typology, the original buildings could be classified in wealthy owner-occupied town houses (*hotel particulier* in French) and blocks of flats for rental (Fig. 2). The first type, seeking a more urban, luxurious and wealthy character, maintained the neoclassical hierarchy of the different floors: the base, formed by the ground floor and sometimes a mezzanine, the *piano nobile*, the main floor which the owner of the building would occupy, and one or two upper floors crowned by an attic or a pitched roof. On the other hand, rental houses were multi-family dwellings with four to six floors and uniform façades with relatively modest architectural decorations and mansard roofs.

The façades' architectural styles are varied, from Academic Eclecticism, Historic Eclecticism, and Neo-baroque Eclecticism (Ajuntament de València 2005) (Fig. 3), to Catalan-influenced Modernism and Viennese-influenced Modernism (Benito 1992b) (Fig. 4).

Nowadays *Pla del Remei* is one of the wealthiest neighbourhoods in the city, where most of the Valencian Modernist heritage is located. However, despite being declared Asset of Cultural Interest in 1993 (Govern Valencià 1993), due to the proximity of this area to the city centre, during the second part of the XX century, many buildings were demolished to be replaced by reinforced concrete structures with "modern" façades increased number of floors and in some cases greater foot print extending over several plots, therefore changing the urban scene (Fig. 5) (Ajuntament de València 2005).

At the beginning of the XXI Century, due to the growing public perception of having reached a critical point in terms of the urgency of preserving some of the environmental characteristics that made this area of Valencia unique, a Special Protection Plan

Fig. 3 Eclecticism style Buildings in *Pla del Remei* quarter. **a** Academic eclecticism, **b** Historic eclecticism, **c** Neo-barroque eclecticism. (*Source*: Authors 2021)
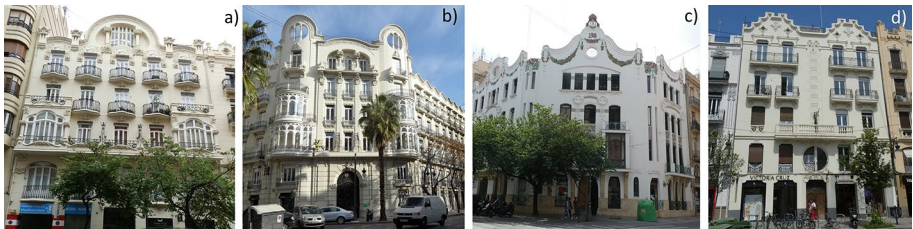

Fig. 4 Modernism style buildings in *Pla del Remei quarter*. **a**, **b** Catalan-influenced Modernism **c**, **d** Viennese-influenced Modernism. (*Source*: Authors 2021)

Fig. 5 New modern buildings in *Pla del Remei* quarter. (*Source*: Authors 2021)

named P.E.P.1 was drafted (Ajuntament de València 2005). Thanks to the approval of this plan, many of the masonry residential buildings built at the end of the XIX century and the beginning of the XX century were saved from the indiscriminate demolitions that took place in the latter decades of the XX century.

3 Methodology

There are three elements of novelty of the methodology proposed in this study: the complete integration of information at different scales from urban to structural, in a unique searchable database indexed for individual buildings; the use of this integrated information to define specific building typologies, tailoring the numerical analysis methods to the typologies identified and seamless use of the data for the fragility analysis, without further
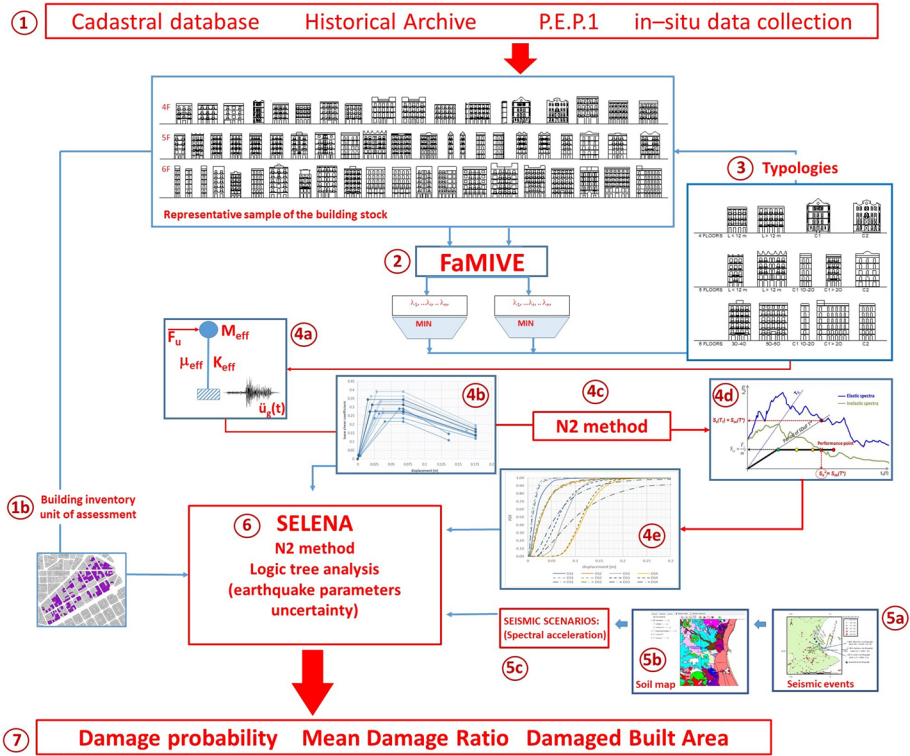
Fig. 6 Procedure for the definition of the capacity curves and fragility functions for selected typologies (FaMIVE), the hazard characterisation and the damage and losses assessment (SELENA)

simplifications; finally the production of risk analyses at the urban scale, but specific to each building unit, including the heritage value of each asset.

This highly interdisciplinary integrated methodology consists of different processes, which together with the flow of data are represented graphically in the flowchart in Fig. 6. The first task is the collation of a detailed building inventory and the creation of an online searchable database which records the currently surviving 205 masonry residential buildings built in *Pla del Remei* area before the end of the Spanish War (1939). (Element (1) in the flowchart of Fig. 6). The information is obtained from different sources, bibliographical, archival, digital, photographic and observational, integrating urban, architectural and structural details. The data is recorded with reference to individual buildings and their facades, and analysed to identify criteria for grouping them which allows to consider a reduced sample of buildings to conduct the seismic capacity and fragility assessment. Due to the limited flexibility of the planning regulations at the time of construction with regard to the number of stories, the height between floors, and the proportion and size of the openings, and considering the reduced structural typologies available at that time, this sample can be considered quite homogeneous. Details on the database construction, data collection and sample selection are provided in Sect. 3.1.

From the database, specific parameters are extracted for each façade and used as direct entry for the FaMIVE analysis method in step 2 (D'Ayala and Speranza 2003, D'ayala

2005, D'Ayala 2013), (see Fig. 6, item (2)). The FaMIVE procedure is based on determining the in-plane and out-of plane strength and displacement capacity of each single façade using a kinematic approach. Its input requires a maximum of about 200 data points per façade, to describe the geometry and material characteristics of the problem, so that the high fidelity of the data collected in step 1 is not lost in the analysis. More details are provided at the end of Sect. 3.1 and a full input form is shown in Fig. 17. The FaMIVE approach is used to determine the collapse load factor and a single degree of freedom equivalent capacity curves for each façade. This is used in an iterative approach whereby the collapse load factor and capacity curve of each building are correlated to both architectural and structural features to determine homogenous typologies, beyond the apparent architectural variety of the façades (item (3) in Fig. 6). This is a novel and essential step to correlate construction details and seismic performance to visual characteristics identifiable from onsite observations, rather than structural parameters, which cannot be readily obtained. According to architectural criteria and defined ranges of capacity, buildings are then classified into separate typologies to each of which corresponds an average capacity curve (item 4c) which can be analysed with the N2 approach (Dolsek and Fajfar 2004, item 4d) to provide corresponding fragility functions for four different damage states (item (4e) in Fig. 6). This process is discussed in greater detail in Sect. 3.2.

Once the typologies are identified, and each building is assigned one, the inventory (see Fig. 6 item (1b)) is also used as direct input to the SELENA platform (Molina and Lindholm 2010 (see Fig. 6 item (6)), by considering each building as a unit assigning to it the corresponding capacity curve and fragility function, as well as the data relevant to soil classification and earthquake intensity measure (see Fig. 6, item 5). Choice of the probabilistic hazard scenarios (item 5c in Fig. 6) and risk model are provided in Sect. 3.3. Output is produced for each building, considering its probability of being in one of 5 damage states (none, slight, moderate, extensive and complete) and its mean damage ratio, while losses are computed in terms of total damaged floor area (item 7 in Fig. 6). These are presented in Sect. 4.

For the Slight, Moderate, Extensive, and Complete structural damage states, descriptions can be found in Hazus Earthquake Model Technical Manual (FEMA 2020) with the detailed attributions for the unreinforced masonry buildings summarised in Table 1. The range of drift limits (%) obtained by comparing the Norme Techniche per le Construzioni NTC 2008 (MIT 2008) and NTC 2018 (MIT 2018), the Eurocode 8 (EC8) (CEN 2004), the American Society of Civil Engineers building code 7 (ASCE 07-16) (ASCE 2016) and the National Building of Canada (NRC 2015), are presented for each damage state, in Table 1.

3.1 Exposure characterization: integrated database construction

A new building database, consisting of the 205 still standing masonry residential buildings built before 1939 in *Pla del Remei* area has been created. The objective of the database is a full characterisation of the construction and structure of each of the buildings and the identification of common architectural features that can be used to correlate construction to seismic response. With this purpose, five different types of sources, with information at different scales, from urban to engineering detail, have been consulted. The data extracted is compiled on an indexed excel workbook, georeferenced by linking the data to the Shape File (SHP) for *Pla del Remei* retrieved from the Cadastral Database (SEC 2022), and visualised spatially by using the GIS open source mapping tool gvSIG (gvSIG association 2009). From this source and through the new GML format of the cadastral database

Table 1 Damage States, correlated visible damage and range of drift limits according to different Standards and for different structural response (shear or flexural), where h_0 is the distance between the section where the flexural capacity is attained and the contraflexure point, l is the in-plane horizontal dimension of the wall or wall pier

| Damage level	Damage evidence (HAZUS Manual, FEMA 2020)	Drift limits (%) (NTC 2008, NTC 2018, EC8, ASCE07-16, NBC2015)
Slight structural damage	Diagonal, stair-step hairline cracks on masonry wall surfaces; larger cracks around door and window openings in walls with a large proportion of openings; movements of lintels; cracks at the base of parapets	0.2–0.3
Moderate structural damage	Most wall surfaces exhibit diagonal cracks; some of the walls exhibit larger diagonal cracks; masonry walls may have visible separation from diaphragms; significant cracking of parapets; some masonry may fall from walls or parapets	0.4 -0.8, $0.8 h_0/l$
Extensive structural damage	In buildings with a relatively large area of wall openings, most walls have suffered extensive cracking. Some parapets and gable end walls have fallen. Beams or trusses may have moved relative to their supports	0.5–1.0 $1.07 h_0/l$
Complete structural damage	Structure has collapsed or is in imminent danger of collapse due to in-plane or out-of-plane failure of the walls. Approximately 15% of the total area of URM buildings with Complete damage is expected to be collapsed	0.7–2.5
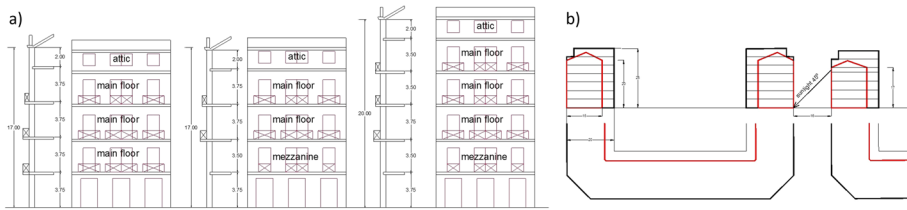
Fig. 7 a Maximum building and inter-storey heights. **b** Changes in height and depth of the buildings. *Source*: The authors

(European INSPIRE directive), the database allows the integrated interpretation of the different data sources and the identification of the relevant typologies.

The history of development of the residential buildings of *Pla del Remei* is traced in the book "El Ensanche de la ciudad de Valencia de 1884" (COAV 1984), a selection of papers analysing the construction of the 1884 Eixample neighbourhood, its evolution, and the surviving buildings, published by the Chartered Association of Valencian Architects (COAV) in 1984, on the occasion of the 100th anniversary of the urban design of this district.

The COAV (1984) includes a copy of the original urban planning regulations. These fixed the maximum number of floors and the inter-storey heights to guarantee ventilation and sunlight. Initially, buildings should have 2 or 3 main floors, with a height of 3.75 m, allowing mezzanines and attics with inter-storey heights of 3.5 and 2 m, respectively. The maximum allowed height for the facades, at the beginning of the development of this area, can be seen in Fig. 7a. However, once the urban development started, pressure on property and land use forced a change of the urban regulations, allowing more built up volume, increasing both the depth of the footprint and the number of floors (black lines in Fig. 7b).

Considering the position of the stair-wells and the ventilation courtyards, notwithstanding the different architectural styles (Eclecticism, Modernism, etc.), and the tenure status (rental or ownership) for the rectangular cadastral units two different layout became most common: one with the staircase next to the party wall serving one flat at each storey, and the other with the staircase in the middle serving one or two flats at each storey (see Fig. 8). Both typologies, with a number of storeys ranging between 3 and 6, and a depth between 15 and 20 m, were adapted to the rhomboidal and pentagonal plots corresponding to the chamfers of the urban block (Fig. 8).

Specific data on each individual building can be obtained through the Cadastral database (SEC 2022) and its online products. Data relating to the geographical position of the buildings, the age of the buildings, the number of floors, building floor area and geometry are shown in Table 2. Importantly, the open access *dxf* files allow to take measurements relating to the building footprint and other details of the façades. Moreover, for each cadastral unit, the Cadastral database includes a photograph of the main façade, allowing a one to one match. These pictures were checked with Google Street View (GSV) and by direct on site observation, where information was contradictory or more external façades are associated to the unit.

Façades, assuming there is not a proper connection to the thin inner walls, have been classified with respect to their position in the urban block as, internal (IN), chamfered side façade (C1) or chamfered central façade (C2) (see Fig. 8), and the number and layout of the openings has been recorded. Linking the open access SEC database with the AutoCAD® files through the Shape File in gvSIG allows mapping and analysing the distribution of data, such as number of floors or architectural style (see Fig. 9).
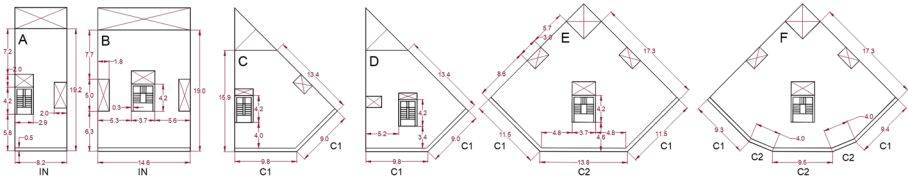
Fig. 8 Common building layouts in *Pla del Remei* quarter and classification of the façades. *Source*: The authors

Table 2 Cadastral database

Data Source	Urban data: Cadastral database (SEC 2022)
DBF: Data Base Files (OpenOffice base)	Nº of floors Age and dates of refurbishments Dimension of the plot Coordinates X, Y (ETRS89 U.T.M. zone 30N)
SEC website: https://www.sedecatastro.gob.es	Number of dwellings Surface area of each dwelling Picture of one façade
SHX: Shapefile shape index format files. (AutoCAD®)	Position whithin the block Number of façades per building Length of each façade can be measured Area of the footprint of the building can be measured
SHP: Shapefile shape format files (gvSIG)	Linking DBF + SHX info

The catalogue of P.E.P.1 Special Protection Plan (Ajuntament de València 2005) contains information useful to identify the architectural style and the grade of listing of each building as can be seen in Fig. 10. This was integrated by an extensive field survey, to identify masonry residential buildings which were not listed, and buildings which did not have an unreinforced masonry load bearing structure. Definition of the different classes of listing and their distribution in *Pla del Remei* are shown in Fig. 11. Of the analysed buildings, 6% are grade I residential listed buildings (buildings of exceptional interest) about a quarter (24%) are grade II and the majority are grade III (61%) while only a minority are not listed (9%). The listing is important as it clearly defines the level and extent of intervention that these buildings can undergo and therefore whether seismic strengthening can be implemented safeguarding their value.

More detailed technical data on the geometry (thickness of the load-bearing walls, dimensions and layout of the openings, inter-storey height, dimensions of the balconies and parapets…) and the structural characteristics (type of masonry, mortar, horizontal structure and roof typology) could be retrieved from 63 original plan drawings dated from 1906 to 1935 of residential buildings deposited at the Municipal Historic Archive of Valencia (AMHV). Sadly, only 27 of the 63 projects correspond to present day existing masonry buildings.

In most cases only a scale drawing of the building plan and elevation showing the thickness of the walls and the dimensions and layout of the openings are available (Fig. 12). In some cases, the drawing of the cross section has allowed to obtain the thickness of the floors and the inter-storey heights. In rare cases, technical drawings were available, allowing the identification of the horizontal structure typology of the original project (Fig. 13a, b). Additionally, as the urban regulations of the *Pla del Remei* changed between the end of the nineteenth century and the beginning of the twentieth century, allowing buildings with greater number of storeys, some of the earlier buildings added one or two story to increase the floor area and hence their commercial value. (Fig. 13c).

Given the sparse information included in the deposited drawing in relation to the structural details, several buildings were surveyed to ascertain their structural typologies. The result of the inspections shows that the structural solutions were very consistent across all buildings and architectural styles, comprising unreinforced brick masonry bearing walls (façades, staircases and party walls), inner brick columns, and one-way horizontal structures with timber or steel beams and joists and light tiles vaults (see Fig. 14).

Construction materials and techniques used in the XIX century in *Pla del Remei* were studied by J.M. Fran in his Phd Thesis (Fran 1990). According to this study, façades were built with load-bearing masonry walls of fired ceramic bricks laid in lime mortar with a thickness of *1 ½ pies*[1] or 2 *pies* depending on the type of bond used, while party walls were one *pie* thick built in stretcher bond as represented in Fig. 15. *Pie* stands for the length of the stretcher, independently of the dimensions of the brick. In the cases under study, the dimensions of the bricks were obtained by in situ measurements.

Figure 16 shows the dimensions measured on the load-bearing wall of the buildings in the area (24 cm long and 5 cm thick) and one of the lintels built with a brick arch *1 ½ pie* thick. These dimensions are consistent with the results published by the researchers of the Municipal Archaeological Service of Valencia (SIAM) about the evolution of the size of bricks with time based on local archaeological surveys carried out. (Altarriba et al. 2001) Their results show that in the period 1890–1939 the length ranged between 260 and 240 mm, the width around 120 mm and the depth between 40 and 50 mm.

Taking into account the description of Fran (1990) and the works of the SIAM (Altarriba et al. 2001) and that there is no evidence that the thickness of the loadbearing wall is related to the number of floors, two possible scenarios, regarding the thickness of the loadbearing façades have been considered: 360 and 480 mm as a result of considering the dimension of the brick units equal to $240 \times 120 \times 50$ mm and the thickness of the façade equal to *1 ½* or 2 *pies*.

Regarding the mechanical properties of the brick masonry, as a Spanish building code did not exist at the time, architects and civil engineers based their designs on recommendations published in the technical journal *Revista Obras Públicas*, (ROP 1903a, b). The values for masonry compressive strength in use in the early twentieth century, published by this journal, compare well to the characteristic compressive strength values (f_{sk}) provided by Eurocode 6, (EN 1996-1, CEN 2005, EN 1996-3, CEN 2006) for class clay bricks and

---

[1] Although "pie/pies" means "foot/feet", in this case corresponds to a traditional construction jargon where "pie" is equivalent to the length of the stretcher of the brick independently of their dimensions. Therefore, "1 ½ pies" means that the thickness of the wall is equivalent to the length of the stretcher of the brick plus the length of the header of the brick, while "2 pies" means that the thickness of the wall is equivalent to the length of two stretchers.
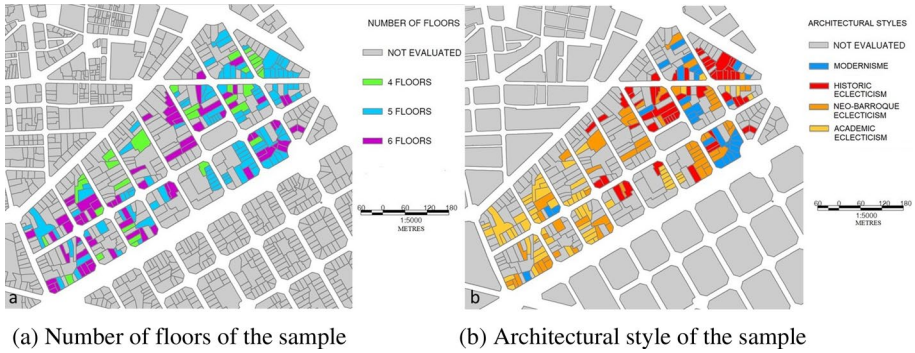
(a) Number of floors of the sample (b) Architectural style of the sample

Fig. 9 **a** Number of floors of the sample **b** Architectural style of the sample
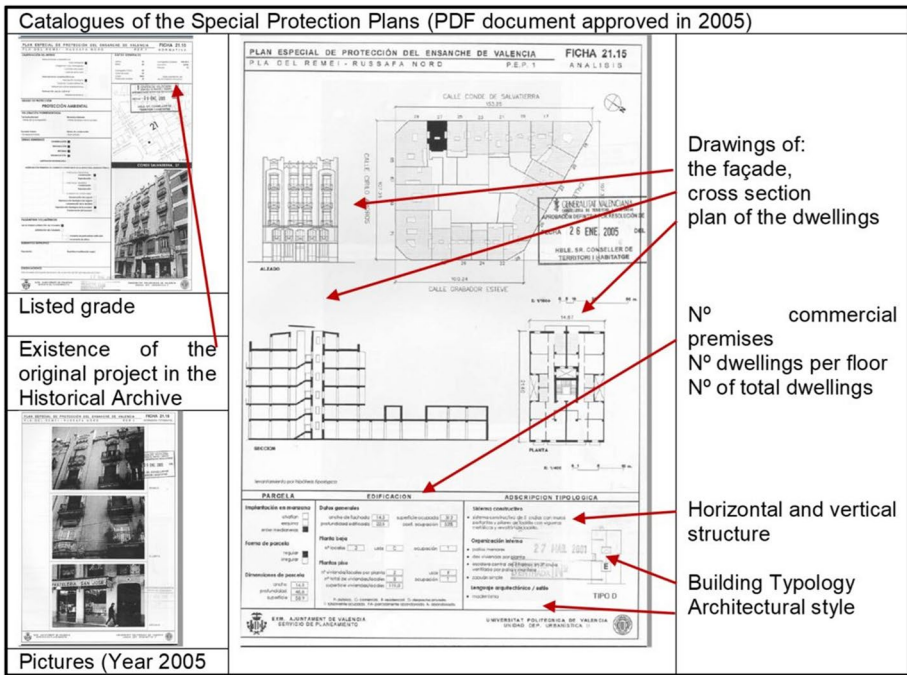

Fig. 10 Catalogue of the Special Protection Plan (P.E.P.1 Ajuntament de València 2005)

M 2.5 mortar. Therefore, the corresponding values suggested by Eurocode 6 (EN 1996-1, CEN 2005, EN 1996-3, CEN 2006) for friction coefficient and cohesion are used in this study.

Timber floors were the norm until 1906, when the first building with steel joists was built in Valencia. According to J.M. Fran (Fran 1990) timber floors and steel floors coexisted until 1910, and from then on, the steel floors typology was predominant. However, the field work has revealed that timber floors can be found in buildings built around 1920, probably due to the scarce supply of hot rolled steel profiles. Therefore, there is no
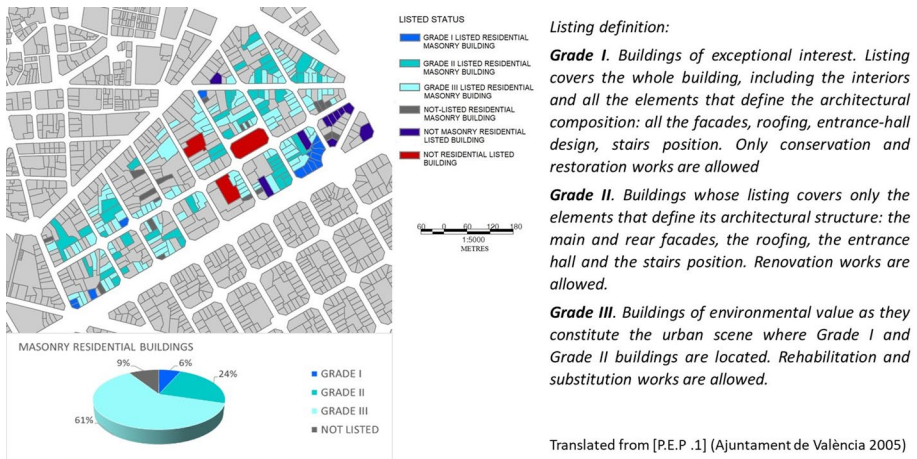
Fig. 11 Listing grades of the buildings in the area. *Source*: The authors according to P.E.P. 1
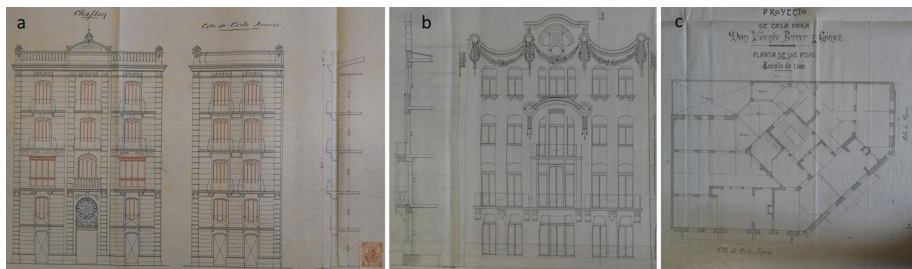
Fig. 12 Original building drawings. **a** façades and cross section. **b** façade and cross section. **c** building plan with load bearing walls. *Source*: Archivo Histórico Municipal de València. **a** AHMV Ensanche 1906 Caja 2 Exp nº 17 C/Cirilo Amorós 23. **b** and **c** AHMV Ensanche1907 Caja 1 (26) Nº 94 EXP 12 H57 RG 4418)

evidence that the material of the horizontal structure, either timber or steel, correlates to the age of the building.

Additional construction detail on the different types of floors existing in the area including their self-weight can be inferred through the Spanish code MV 101 (Ministerio de la Vivienda 1963) and studies by Diodato et al. (2015). Three types of floor structure were identified through the survey: (A1) Timber joists with lightweight tile vaults with an average weight of 3 kN/m², (B) Steel joists with lightweight tile vaults and a weight of 3.5 kN/m² and (B1) Timber joist with lightweight tile vaults and thin reinforced concrete slab for the buildings that have been refurbished, weighing an average 4 kN/m².

In terms of the stiffness, these floors cannot be considered as infinitely stiff in their plane, therefore, for the structural analysis they are assumed as flexible structures with limited ability to redistribute mass to orthogonal sets of walls. As shown in an experimental work by Maheri et al. (2012), the original system is able to develop very modest 2-way behaviour, impaired by longitudinal cracks at the interface between tiles and joists. The introduction of the concrete slab, conversely, does prevent such cracks, and therefore increases somewhat strength and ductility, but increases also the mass of the system by up
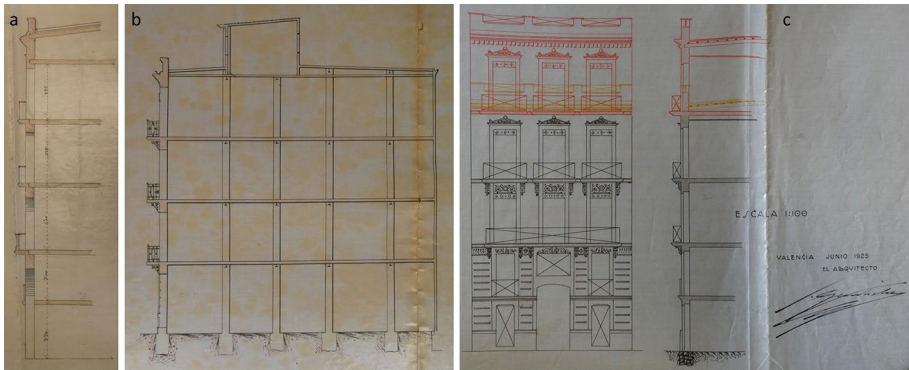
Fig. 13 **a** Cross section with timber joist. **b** cross section with steel beams. **c** Addition of one storey in an existent building. (*Source*: Archivo Histórico Municipal de València. **a** AHMV Ensanche 1906 Caja 2 Exp RG 1023 C/Conde Salvatierra 2. **b** AHMV Ensanche 1925 C/Cirilo Amorós 81. **c** AHMV Ensanche1925 caja 2 H528 Cirilo Amorós 34)

Fig. 14 Structural typologies: **a** timber beams and joists, **b** brick masonry bearing wall and timber joists, **c** brick masonry column with steel beams and joist and d) steel beams and light tiles vaults. (*Source*: Authors 2021–2022)

to 33%, without developing full composite action. Finally, regardless of whether the floors were built with timber or steel joist, the roof were always built with timber joists, rafters, reeds with mortar and curved Arabian roof tiles. The total mass is substantially lighter than the floor mass at 1.5 kN/m^2.

Another issue to be considered is the presence or absence of timber tie beams or wall plates at each floor level. According to Fran (1990) the joists, usually orthogonal to the façade, rested at one end on the internal beams, (see Fig. 14a) while the other end rested
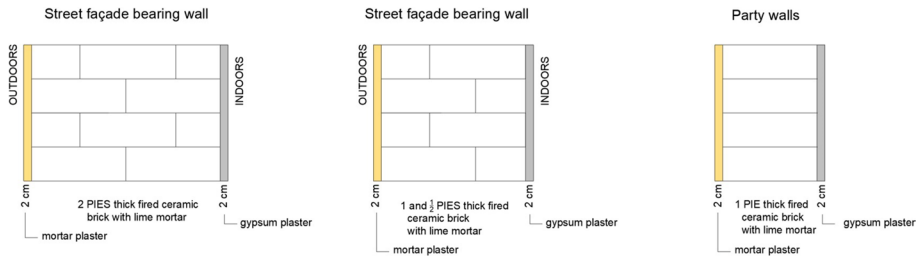
Fig. 15 Original bearing walls bond and thickness according to J.M. Fran (Drawn by the authors)

directly into pockets created in the bearing brick walls (see Fig. 14b). This constructive solution, with putlogs for the joists, was the cause of several constructive pathologies (Fran 1990). A similar arrangement applies to the rafters, which at one end sit on the ridge beam and at the other end are inserted into the load-bearing façade, without, in most cases, the use of a tie beam. However, despite Fran's statement, evidences of what seems to be timber tie beams have been seen during fieldwork.

The outcome of this integrated analysis provides the criteria to select a representative sample of the 205 buildings available to conduct the analytical seismic vulnerability assessment. While it would have been feasible to analyse each of the buildings in *Pla del Remei,* the purpose of this step is to show that representative samples can be identified for assessment of much larger building stocks, and that sensitivity analysis can be conducted on uncertain parameters instead. The ultimate objective of this approach is to identify a relatively small number of typologies to bring forward in the risk analysis balancing simplification with specific seismic response.

Therefore, the criteria for selection are:

- Prioritize buildings with reliable information about the geometric dimensions both global and detailed, as it can be retrieved from the original projects or the Special Protection Plan P.E.P. 1;
- Proportional representation in the sample of the different number of floors, i.e. buildings with 4, 5 or 6 storeys;
- Proportional representation of buildings with different numbers of opening, as observed in the building stock, from one vertical alignment of windows, up to six in the wider facades. Because the size of the openings and the size of the piers are relatively regular across the building stock, this criterion, together with the previous one, provides a wide range of facades with different slenderness. It should be noted that there is no correlation between the number of openings and the number of floors.
- Proportional representation of the façade position in the block, as discussed with respect to Fig. 8. Specifically, distinction is made between façades along the sides of the block, which are connected with side and party walls at 90° (IN) and facades corresponding to the chamfers of the block, which are connected to other portions of the façade with angles wider than 90° and they either have one connection with a side wall (C1) or none (C2) if they are central to the chamfer, as thin inner walls cannot be considered properly connected with the façades. These geometries affect the level of connections in the masonry fabric and the restraint offered by the side walls to the façade to prevent out-of-plane failure.

Fig. 16 Dimensions of the brick units and thickness of the façade. (*Source*: Authors 2022)

Considering the above-mentioned criteria, the representative sample for the seismic analysis accounts for 43 existing buildings and their 59 façades. Given the proportion of different number of storeys and positions of the façades in the block, this sample size provides a confidence level of 85% and a margin of error of 15% for the number of buildings and a confidence level of 90% and margin of error of 10% for the façades. These values are acceptable given the confidence levels related to the hazard. The uncertainties related to other structural characteristic, such as thickness of the façades, floors typology and existence of tie beams, for which a robust statistical distribution within *Pla del Remei* quarter could not be ascertained, have been accounted for through sensitivity analysis by assessing each façade several times, assuming the possible permutations of the options included in Table 3, and analysing their influence on the collapse load factor, the vulnerability class and the failure mechanisms.

The database records for the 43 buildings have been used as input to FaMIVE, which has been customised to represent the specific architectural characteristics of this building sample, by specifying the horizontal structures characteristics, taking into account the additions above the 5th and 6th floor, the variability in storey heights, and the state of conservation for each façade (Fig. 17). The latter is explicitly surveyed in FaMIVE by providing three qualitative classes (bad, medium, good conservation state, parameters 5.7a–5.7c), then accounted for in the calculations by reducing the effective thickness of the walls, depending on the attributed class. FaMIVE also accounts for the reliability of the data collected, by considering three classes of margin of error in input, between 5 and 15%, depending on the data source and collection method. A reliability function is then employed to determine the margin of error of the output.

3.2 Typologies identification and fragility analysis

The FaMIVE approach (D'Ayala 2013) is composed of two parts: a limit state analysis routine which identifies the most probable collapse mechanism (out of 23 possible ones) and its corresponding load factor for a given façade with given edge constraints and loading conditions, and a fragility analysis routine. The latter, based on the modified N2 method approach (Dolsek and Fajfar 2004) require first to derive simplified capacity curves, which is accomplished by treating the collapsing portion of the façade as a nonlinear single degree of freedom (SDOF) oscillator. The mass of the SDOF oscillator is determined by the façade's volume and the tributary area of the horizontal structures activated in the mechanism; its stiffness is determined by the geometry of the same portion, the type of mechanism and its constraints, using canonical stiffness equations for walls in lateral shear and flexural deformation. Mass and stiffness as derived above are used to determine the

Table 3 Permutations of the structural characteristics considered to account for uncertainties in the construction typologies

Thickness of the bearing façades	360 mm (1 ½ pies)
	480 mm (2 pies)
Type of floors	Timber floors
	Steel floors
	Strengthened floors
Existence of tie beams	Yes
	No

Fig. 17 FaMIVE inspection form

fundamental period T of each oscillator. Finally, the ductility of the SDOF nonlinear oscillator is defined by using a stability criterion, whereby the geometric parameters of the façade determines its loss of equilibrium. (see D'Ayala 2013; Novelli et al. 2015, Sorrentino et al. 2017, for a full treatment of the approach and its application).

Applying this procedure, an idealised linearized capacity curve corresponding to each façade is obtained. considering for each curve the specific performance thresholds corresponding to slight, moderate, extensive and complete damage. In Fig. 18, such curves are plotted grouped for number of storeys. Each set collates the option for alternative type of horizontal structure, alternative nominal thickness of the façade, and presence of timber tie beam or wall plates, resulting in 192 facades for the 5 storeys and 6 storeys groups and 144 facades for the 4 storeys group for a total of 528 cases analysed. It can be seen that there is substantial variability of stiffness and strength capacity, with the 5 storeys façades showing the highest dispersion. The base shear coefficient, computed as the ratio
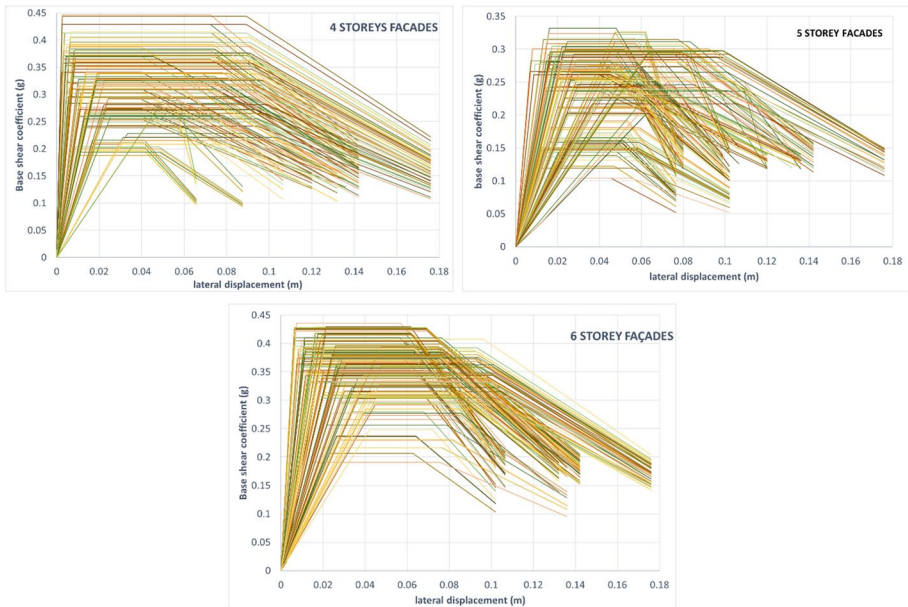
Fig. 18 Sets of capacity curves for all the 4, 5 and 6 storey façades

of the lateral force resisted to the mass of the façade and expressed in units of (g), ranges from a minimum of just above 0.10 g for a 5 storey façade developing a local overturning collapse mechanism (upper triangular portion of the façade in presence of tie beam), to a maximum values just below 0.45 g for a 4 storey façade with good connections with the side walls developing an out of plane failure mechanism, where part of the side walls are also mobilised.

The range of lateral displacement corresponding to the four performance thresholds are similarly highly affected by the individual conditions of each façade and the specific mechanism that it develops. The drift is computed as the ratio of the displacement at the centre of gravity of the façade to its height above ground. The range of damage thresholds' drift obtained with the numerical analysis for each damage state are compared in Table 4 with the range of drift limits provided by the standards as outlined in Table 1. It can be noted that the computed damage threshold's drifts are generally lower than the corresponding limits prescribed by the standards, especially for lower damage states, highlighting the comparatively high stiffness.

Homogeneous subsets of curves were created for number of storeys, presence/absence of tie beams and nominal thickness. For each of these a multivariate analysis was conducted considering the influence of the position in the block, number of openings, length of the façade and façade's slenderness, pier slenderness, on the resulting performance. Specifically, the range of collapse load factors and prevalent collapse mechanism were used to further identify homogeneous subsets. Ultimately façades were grouped by position and length which in the case of 6 storey facades, also correlated to the number of openings. Therefore, 14 different typologies representing the building stock of *Pla del Remei* quarter where finally identified (Table 5). For each of them 4 different construction assumptions, with and without tie beam and the two different nominal thicknesses are considered,

Table 4 Comparison between computed drift at the 4 performance thresholds and code recommended drifts (see Table 1)

| | Slight damage | | Moderate damage | | Extensive damage | | Complete damage | |
	Computed (%)	CODE ref (%)	Computed (%)	Code ref (%)	Computed (%)	Code ref (%)	Computed (%)	Code ref (%)
Minimum	0.0011	0.2	0.05	0.4	0.39	0.5	0.74	0.7
Average	0.025		0.196		0.73		1.28	
Maximum	0.1	0.3	0.64	0.8	0.95	1	1.54	2.5

Table 5 Façades typologies

	Inner façade		Chamfered side façade		Chamfered central façade
4 Floors	Length < 12 m 4B-4F-L ≤ 12	Length > 12 m 4B-4F-L > 12	All openings 4B-4F-C1		Any number of openings 4B-4F-C2
5 Floors	Length < 12 m 5B-5F-L ≤ 12	Length > 12 m 5B-5F-L > 12	1 or 2 openings 5F-C1-(1O&2O)	More than 2 openings 5F-C1-(3O)	Any number of openings 5F-(C2)
6 Floors	3 or 4 openings 6B-6F-L ≤ 12	5 or 6 openings 6B-6F-L > 12	1 or 2 openings 6F-C1-(1O&2O)	More than 2 openings 6F-C1(6O&4O)	Any number of openings 6F-(C2)
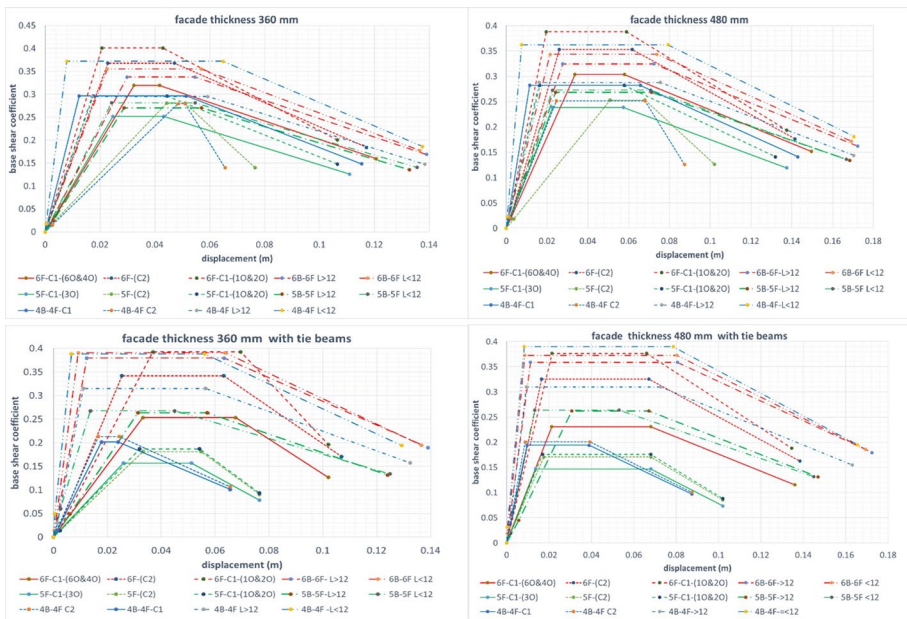
Fig. 19 Average capacity curves for the 14 building typologies for the two sizes of thickness and presence/absence of tie-beams

leading to a total of 56 typologies, to be used for the fragility analysis. The capacity curves obtained for these typologies, representing the average response of each subset are shown in Fig. 19. It can be seen that the variability in strength, stiffness and ductility is preserved within each subset, as well as the evident difference in performance across the four subsets. Particularly, while the presence of the tie beams generally results in an increase of stiffness of the system, and some time an increase in ductility, this not always correspond to an increase in strength as, while the global mechanism is prevented by the presence of the tie, a local mechanism can be triggered with a relatively low collapse load factor.

The fragility assessment represents the next step in the methodology to determine the seismic response of these building types. Among various methods of deriving fragility

functions, the N2 method (Fajfar 2000) incorporated in Eurocode 8 (EN 1998-1 2004, CEN 2004) is adapted here by using idealised bilinear capacity curves, one for each of the curves in Fig. 19 against natural response spectra in the acceleration-displacement response spectral space (ADRS) to identify performance points as coordinates of the intensity measure (IM) and engineering design parameter (EDP) (Dolsek and Fajfar 2004).As discussed in greater detail in Sects. 3.3.3 and 3.3.4 the current database of record accelerograms for Spain and the Valencia region specifically, is rather insufficient to the statistical requirements underlying the derivation of site specific fragility functions. Moreover, the typologies considered are applicable, not just to other cities in Spain, but also to other parts of southern Europe, characterised by different seismicity. Therefore, following the approach by (Bozorgnia et al. 2014), the response spectra of the far-field ground motion record suite provided by FEMA P 695 (FEMA 2009) are used in this study, thereby including record-to-record variability. This suite of ground motions is scaled with Sa(T) values ranging from 0.02 to 2.5 g, so that sufficient data points are obtained for fitting lognormal fragility functions corresponding to all the damage levels considered. To be compatible with the SELENA input requirements, in this study fragility functions are generated in terms of displacement. Fragility functions are computed assuming that a given level of damage, light (DS1), moderate (DS2), extensive (DS3) and collapse (DS4), is attained when the structural model response exceeds a certain performance threshold in terms of an EDP of interest (lateral displacement in the present case), given a value of the intensity measure IM (in this study Sa(T1)). Given a cloud of performance points, obtained with the N2 approach, log-linear regression models can be employed to determine the relationship between the EDP and the IM using the total probability theorem. A complete treatment of the method is beyond the scope of this article and can be found in together with a comprehensive literature review on fragility functions derivation and limits of various approaches (D'Ayala et al. 2015).

The fragility functions for the 4 performance levels and for the 56 typologies are presented in Fig. 20 grouped in the four different subsets of thickness and presence of tie-beams. The graph shows that the difference in performance between the typologies is preserved, especially for the advanced performance level of extensive damage and collapse. The idealised capacity curves and the parameters representing each fragility functions are used as input for the risk analysis and computation of losses, performed in SELENA.

3.3 Hazard scenarios and loss computation procedure

The SELENA software (Molina et al. 2010) has been used to compute damage and losses scenarios using the spectral displacement approach in agreement with the N2-method. The methodology requires a building inventory, the soil characterisation to consider site effects and the definition of meaningful earthquake scenarios, besides the capacity and fragility functions derived with the FaMIVE procedure, that are used to obtain the damage probability and damage and loss distributions.

SELENA has the flexibility to choose the scale at which damage and losses are computed. Typically, in regional and urban studies, the unit of assessment represents municipalities, districts or, at the smaller scale, urban blocks. Given the high level of resolution of the present study, whereby a large number of individual assets are considered, the damage and losses are computed for each building in the *Pla del Remei* quarter, each being assigned one of the typologies identified in the previous section.
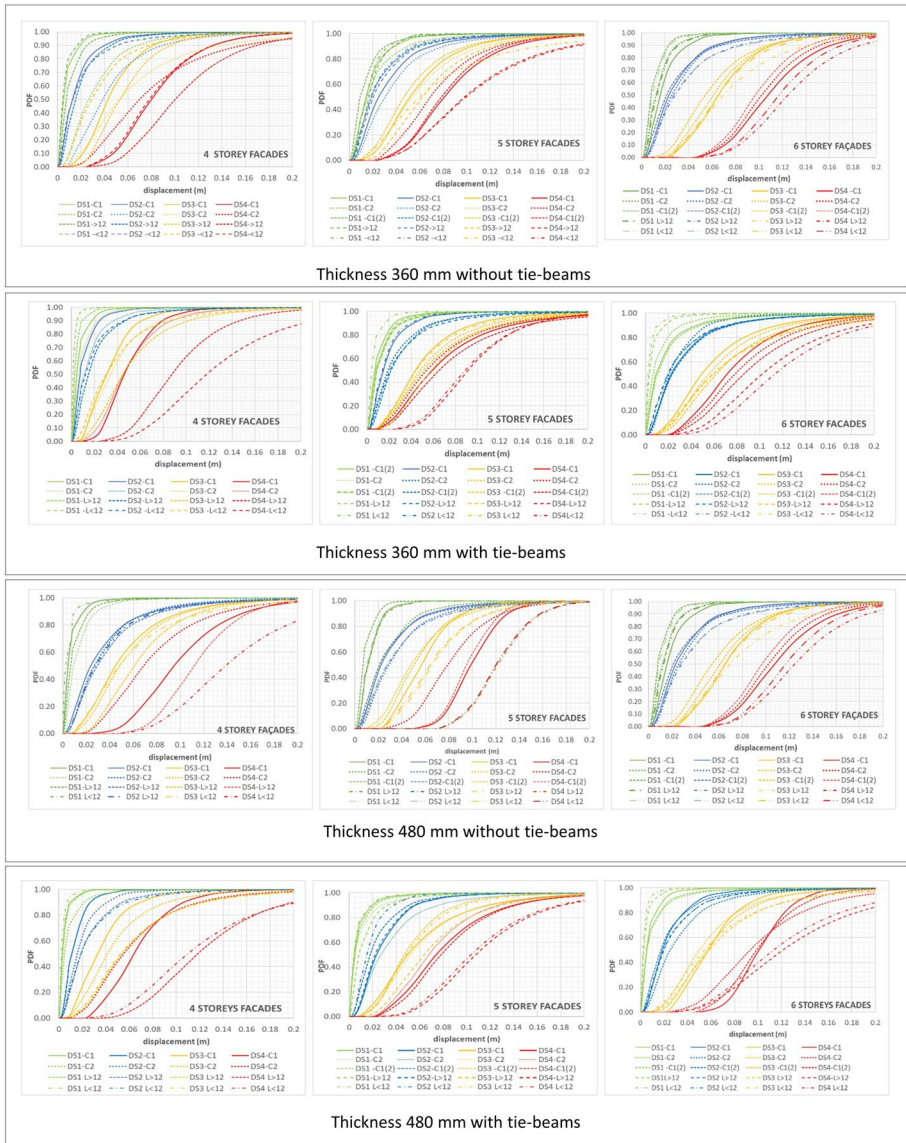
Fig. 20 Fragility functions for the building typologies and constructive assumptions

3.3.1 Building inventory

The building inventory database is one of the needed input files for SELENA, whereby each entry in the database is represented by a geounit. In order to account for buildings at chamfers with more than one façade, for which is not possible to predetermine which one would define the building's vulnerability, the original building inventory has been expanded by including the multiple facades, resulting in a total of 287 elements. The
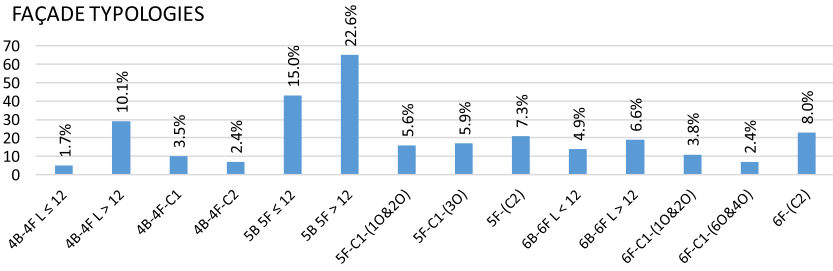
Fig. 21 Façade typologies distribution in *Pla del Remei* area

distribution of the different typologies among the database is shown in Fig. 21. Capacity curves and fragility functions for each building typology are the ones obtained with FaMIVE in the previous section (Figs. 19 and 20 respectively).

3.3.2 Soil maps

The characteristics of the soil at each building plot have been obtained from the Geoweb project website (FIVE 2012). Geoweb is a collaborative project funded by the Spanish Ministry of industry and developed by the Cartographic Institute and the Building Institute of the Valencian Community to provide free information about the expected type of soil at a given geographic coordinates, based on geotechnical studies done by the Valencian Community over the years.

According to the Geoweb tool (Fig. 22), the soil underlying *Pla del Remei* area is fairly consistent, described as medium-dense clay, sand and gravel. Considering the ground classification provided by the clause 3.2.1. of the Eurocode 8 (EN 1998-1 2004, CEN 2004) the soil could be classified as type C ($180 < Vs30 < 360$ m/s) or D ($Vs30 < 180$ m/s) where Vs30 is the time-averaged shear-wave velocity (Vs) to a depth of 30 m. Additionally, Heath et al. (2020) proposed a topographic-slope-based Vs30 value of 300 m/s for this area so, ultimately, a soft soil type C was assumed for the analysis.

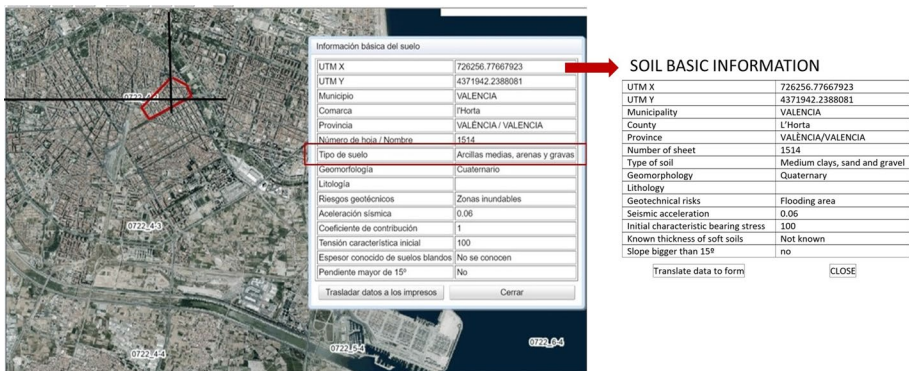**Fig. 22** Soil classification (in Spanish and translation). *Source*: Geoweb (FIVE 2012)

3.3.3 Seismicity of Valencia region and compatible scenarios for Valencia municipality

The Iberian Peninsula shows a low to moderate seismicity in the world context with frequent earthquakes of moment magnitude (Mw) generally smaller than 5.5, although, historically, large damaging earthquakes have occurred with epicentral macroseismic intensity (I_0) IX-X in the EMS-98 scale (Grünthal 1998), as those of 1829 Torrevieja (Alicante) and 1884 Arenas del Rey (Granada). Both earthquakes caused the collapse of many buildings and a high number of human losses (Vidal 1986).

Although the Alicante province is the area of the Valencian region with highest seismic activity rate and record of damaging earthquakes (see Fig. 23a), the Valencia province has also been affected by significant historical earthquakes. The 1396 Tavernes earthquake, with an assigned EMS-98 intensity between VIII-IX was widely felt along the region. It caused extensive damage to buildings, churches and castles, triggering the almost total destruction of the localities of Alzira and Tavernes (Galbis Rodriguez 1932). Damaged buildings were also recorded in the Valencia municipality. No casualties were reported. Martínez Solares and Mezcua (2002) assigned a Mw 6.5 to this event. The 1748 Estubeny earthquake produced extensive damage to buildings, churches and castles with almost total destruction of the locality of Montesa and other towns in the epicentral area (Galbis Rodriguez 1932). It was felt at locations 40–75 km from the epicentre with intensity V (EMS-98), hence it is assumed to have caused no damage in the Valencia municipality.

In the SE of Spain onshore active deformation and seismicity are mainly located along the Eastern Betic Shear Zone (EBSZ), a major strike-slip tectonic corridor belonging to the Betic Internal Zones (see Fig. 23b). Regional and local geodetic studies indicate that the EBSZ is absorbing between 0.2 and 1.3 mm/yr, i.e. only a portion of regional deformation (Martin-Rojas et al. 2020). Martin-Rojas et al. (2020) state that part of this deformation not absorbed by the EBSZ is accommodated in the eastern Betic External Zones, located to the north of the EBSZ, where several major historical earthquakes occurred (e.g., the
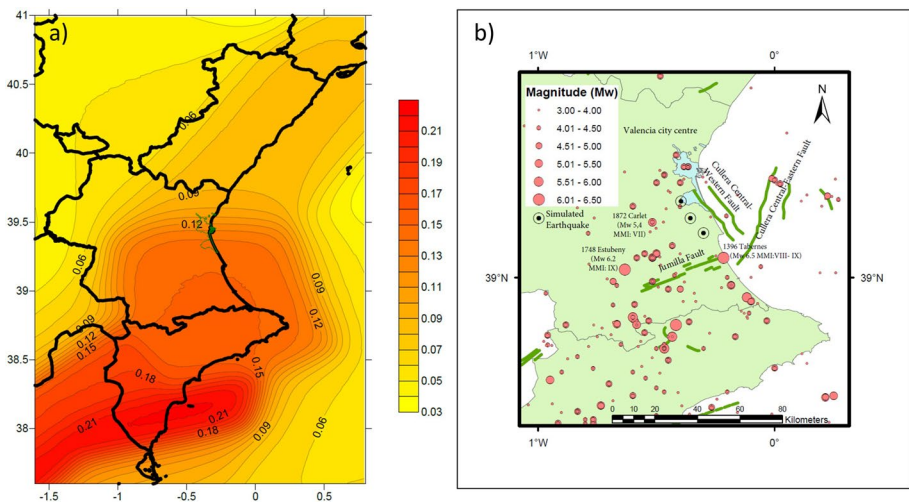

Fig. 23 **a** Seismic hazard (PGA in units of gravity) map for 475 years return period (modified from Kharazian et al. 2021). **b** Seismicity in the Valencia province (Mw ≥ 3.0). The main historical earthquakes are labelled in the map. The light blue area represents the municipality of Valencia. The black circled dots are the epicentral location of the simulated earthquakes (From north to south are Eqs. 1–3)

1396 Tavernes and the 1748 Estubeny earthquakes). Perea (2006) and Perea et al. (2012) propose the Cullera Fault as the possible source of the Tavernes earthquake, while Giner-Robles et al. (2014) and García-Mayordomo et al. (2012) attributed these major earthquakes to the Jumilla Fault.

Additionally, Kharazian et al. (2021) carried out an update of the seismic hazard in Spain as part of a risk-targeted research in the country. The new seismic hazard maps (Fig. 23a) indicate a PGA between 0.10 and 0.14 g for the municipality of Valencia for a return period of 475 years and the corresponding disaggregation indicates that the higher probabilities come from moderate magnitude earthquakes (5.0–5.5) at epicentral distances compatible with the Cullera Western Fault (Fig. 23b). For a return period of 975 years, the corresponding disaggregation also indicates Cullera Western Fault as the epicentre of the event. Additionally, geological studies indicate that probably this fault was responsible for the 1396 Tavernes earthquake.

Therefore, to simulate the impact of probable earthquakes in *Pla del Remei* area for return periods of 475 and 975 years, corresponding to the life safety and collapse prevention limit states, the occurrence of events generated by the Cullera Western Fault with a focal depth of 10 km and magnitudes of Mw 5.25 ± 0.25 and Mw 6.25 ± 0.25, respectively, have been chosen. In addition, three different epicentral location for the fault rupture are considered. Figure 23 shows the seismicity of the area, the active faults, and the chosen epicentral location. Finally, to account for the uncertainties about the magnitude, a logic tree approach is used for each event, attributing probabilities of 0.30, 0.40, 0.30 to the Mw 5.00, 5.25 and 5.50 and 6.00, 6.25, 6.5, respectively, for the two return periods, to compute damage and losses. A higher weight was given to the central magnitude since the maximum PGA in the municipality is similar to the PGA from the seismic hazard map for the corresponding return period. Table 6 summarized the six scenarios used for damage and losses computation with the corresponding variability in magnitude and maximum computed PGA for each case.

3.3.4 Ground motion prediction equations (GMPEs)

Once the epicentre location and magnitude have been defined, a ground motion prediction equation is needed to determine the peak ground acceleration and spectral acceleration shake map, considering magnitude, distance from source to site, focal mechanism, soil type, etc. Currently, the database of accelerograms recorded on Spanish territory by the Spanish national geographic institute (IGN) does not contain sufficient information to fit specific ground motion prediction models so it is usually accepted to employ European or worldwide models. For example, for the current seismic hazard maps of Spain (IGN 2017), a statistical residual analysis using the method proposed by Scherbaum et al. (2004) was

Table 6 Magnitude and maximum PGA values (in units of g) in *Pla del Remei area* for each epicentral location and return period			
Return period: 475 years	Mw = 5.0	Mw = 5.25	Mw = 5.5
Earthquake 1	0.09	0.11	0.15
Earthquake 2	0.04	0.05	0.07
Earthquake 3	0.03	0.04	0.05
Return period: 975 years	Mw = 6.0	Mw = 6.25	Mw = 6.5
Earthquake 1	0.24	0.29	0.33
Earthquake 2	0.12	0.15	0.19
Earthquake 3	0.09	0.12	0.16

carried out to verify the validity of available GMPEs model for specific regions, concluding that for shallow seismicity regions the GMPE proposed by Akkar and Bommer (2010) and the one proposed by Cauzzi and Faccioli (2008) were the most adequate.

Hence the Akkar and Bommer (2010) GMPE is used in this study to compute the ground motion distribution at *Pla del Remei* quarter. This functional form uses the moment magnitude, the Joyner-Boore distance, two coefficients S_A and S_s which are 1.0 for stiff and soft soils or 0.0 for rock (Vs 30 > 750) and assume two coefficients, F_N and F_R, relating to the faulting type so F_N is 1.0 for normal faults and 0.0 otherwise, and F_R is 1.0 for reverse faults and 0.0 otherwise. Then, the information obtained in Sect. 3.3.2 indicates us to assign to S_A and S_s the same value (1.0) and the scenario earthquakes chosen in Sect. 3.3.3, related to the Western Cullera Central Fault, allows us to fix F_N to the value 1.0 (normal fault, as indicated by Garcia-Mayordomo et al. 2012) and F_R takes the value 0.0.

4 Targeted seismic risk assessment

SELENA calculates the damage probability for the five damage states (none, slight, moderate, extensive and complete) for each scenario, including median, 16% and 84% percentile values for each earthquake.

Figure 24 shows, for each typology, construction hypothesis and return period, the maximum and minimum values of the probability of reaching each damage state computed across the 3 scenarios for epicentral location and combination of magnitudes. For the 475 yr return period, it can be observed that façades with capacity curves with higher stiffness tend to have higher proportion of slight damage, as they are more sensitive to small displacements. Therefore, the chamfers façades C2 appear to have slightly better performance than others, in terms of minimum probability of damage. It is also evident that the five storeys typologies are at greater risk of damage than the others. For typologies without tie beams, the case with higher thickness deliver better performance than the case with lower thickness. The effect of the tie beams is less clear, as it shows less difference between minimum and maximum damage probabilities with respect to the cases without tie-beams. However, the results show an increase in the probability of higher damage level in some cases. This can be ascribed to the development of local collapse modes. For the 975 yr return period, the results are influenced by the reserves of ductility of the different typologies, with a marked greater probability of higher damage levels for the façades in chamfers. Façades with greater thickness overall have less probability of damage than slenderer facades, with 4 storeys façades showing the best performance across all typologies. It is also noticeable that the tie-beams appear to be effective in reducing the probability of higher damage level for the hypothesis of thinner walls, when considering a 475 years return period. For 480 mm case, the presence of tie beams prevents some failure mechanisms switching to others involving a bigger proportion of the façade, and therefore, most damaging.

Additionally, SELENA calculates the Mean Damage Ratio (MDR), a useful parameter to highlight the compounded risk for each unit. MDR is defined as the sum of the repair cost corresponding to each damage state expressed as a ratio of the cost of new construction (FEMA 2003), over the number of damage states. MDR values for each typology in each scenario are shown in Fig. 25. These results highlight the influences of the epicentre location for the higher return period since the probability of damage is clearly amplified for the more vulnerable typologies when considering the northest location of the epicentre. The higher probability of damage of facades in chamfers is confirmed within
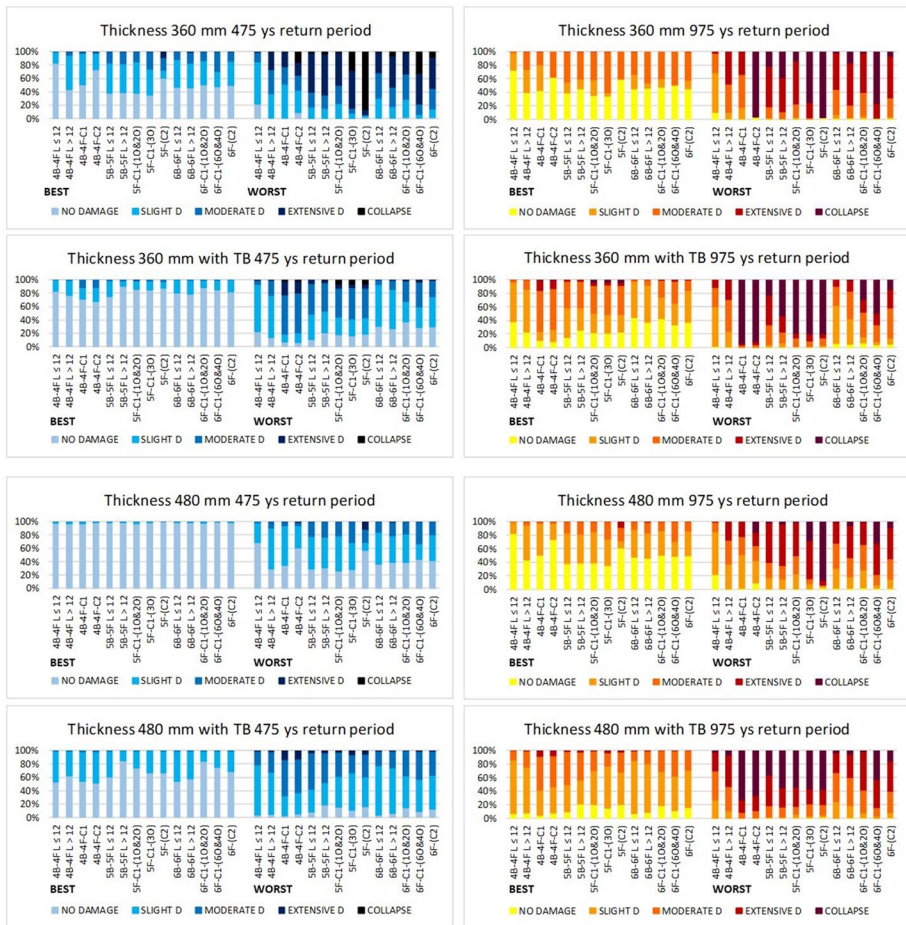
Fig. 24 Best and worst performance prevision considering the probability values of reaching each damage state, for each constructive assumptions, building typology, and seismic scenario

different construction hypothesis and number of storeys, for both return periods, with a MDR close to 1 for C2 façades with 4 and 5 storeys in the case of lower thickness.

In order to have a more detailed picture about the probable economic losses, the expected built damaged area has been calculated.

Direct economic losses depend on the probability of occurrence of each damage state and the repair (mostly for damage states slight and moderate) and replacement (for damage states extensive and complete) costs. Considering that the building inventory is provided in terms of floor area of the buildings, it is possible to estimate the total economic losses caused by the structural and non-structural damage in terms of the built area damaged.

The repair and replacement costs associated with Slight, Moderate, Extensive and Complete structural and non-structural damage can be defined as fractions of the full replacement cost of the building. Hazus Earthquake Model Technical Manual (FEMA 2020), provides the repair cost ratios (in % of building replacement cost) for multi-family dwelling shown in Table 7.

Fig. 25 Mean Damage Ratio (MDR) median values for each constructive assumption and seismic scenario

However, in *Pla del Remei* area the decoration of the façades of the masonry buildings acquires special importance (see Fig. 26), as for the bourgeoisie of the late 19th and early twentieth century, the sumptuous and elaborate coatings, with richly detailed ornamental patterns and mouldings of the façades, were a sign of their social status (Miján et al. 2011). Therefore, considering the heritage value of the buildings in the area, the relative values of the non-structural components, like the exterior plasters of the wall panels, in relation to the overall building replacement value should be increased when taking into account the cost of the decorations, renderings, stuccoes, etc. that characterised the façades of this area.

To evaluate this additional replacement cost, a market survey has been carried out, comparing the market price provided by the "*idealista*" real estate website (Idealista 2022) for masonry buildings built before 1939 and reinforced concrete buildings built after the end of the Spanish Civil War in the same area. The price per square meter (sqm) of a small sample of the buildings reviewed can be seen in Fig. 27, showing that the masonry buildings are on average up to 50% more expensive.

In this proposal, the authors are fully aware of the reliability of this study, since one of the main characteristics of real estate is that it is "unique", i.e. no two properties are ever the same. This situation complicates the comparison and justifies the dispersion of prices in the market, both for masonry and concrete buildings.

Table 7 Structural and non-structural repairs cost ratios according to FEMA 2020 and proposal

Costs ratios in % of building replacement cost	Slight	Moderate	Extensive	Complete	Slight	Moderate	Extensive	Complete
Structural repair costs	0.3	1.4	6.9	13.8	0.3	1.4	6.9	13.8
Acceleration-sensitive non-structural repair costs	0.8	4.3	13.1	43.7	0.8	*19.3*	13.1	43.7
Drift-sensitive non-structural repair costs	0.9	4.3	21.3	42.5	0.9	4.3	21.3	42.5
Total	2	10	41.3	100	2	*25*	41.3	100

Fig. 26 Decorations in *Pla del Remei* Masonry buildings. *Source*: The Authors

Fig. 27 Market prices for masonry and reinforced concrete building in the area. (Data from Idealista 2022)

Furthermore, usually, the character of a listed building does not necessarily imply a higher valuation from an economic point of view, at least in terms of market prices and willingness to pay from prospective buyers. Indeed, the listed status is often perceived as a hindrance due to restrictions on improvements or renovations, which can weight down the sale price of the asset. Moreover, there is no doubt that the repair, refurbishment or replacement of listed buildings (minor heritage) can be considerably more expensive if traditional techniques are used.

Therefore, assuming that the façade account for about 30% of the building cost, the repair cost for moderate damage in acceleration-sensitive non-structural elements has been increased by 15%, with the final costs ratios considered to obtain the built damaged area (BDA) shown in Table 7.

The minimum and maximum proportion of BDA obtained for each return period and construction hypothesis are shown in Fig. 28, where they are divided by listed status. It can be seen that, the minimum values for the 475yrs return period, provide a virtually undamaged outcome for all construction hypotheses, however the BDA could be up to 12% of the total built up area if the maximum value are considered in the case of 360 mm thickness without tie beams. For the 975yrs return period damage could affect more than 50% of the built up area in the case of 360 mm thickness without tie beam and for the 480 mm thickness with tie-beams.

Finally, the minimum and maximum percentages of the expected built damaged area (BDA) have been mapped for the most likely construction assumption (façades 480 mm thick without tie beams) considering both, 475 and 975 years return periods. For the buildings in the chamfers, with more than one façade, the assigned values correspond to the façades with the best and worst behaviour (Figs. 29, 30, 31 and 32).
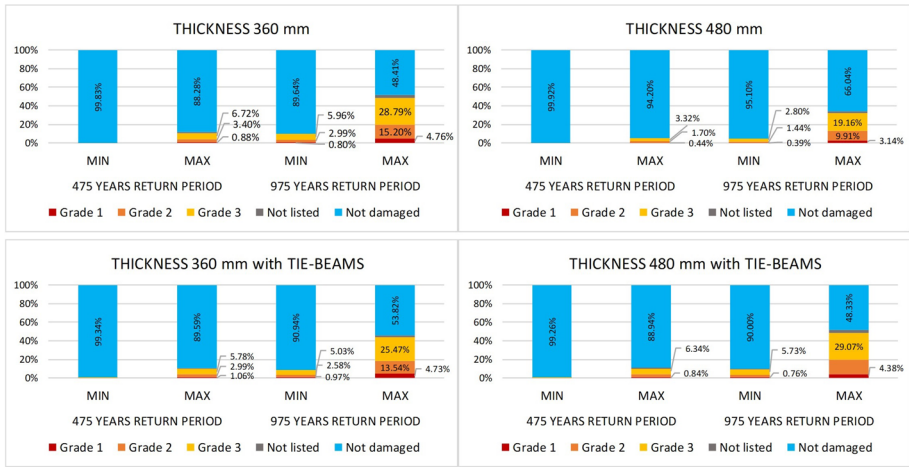
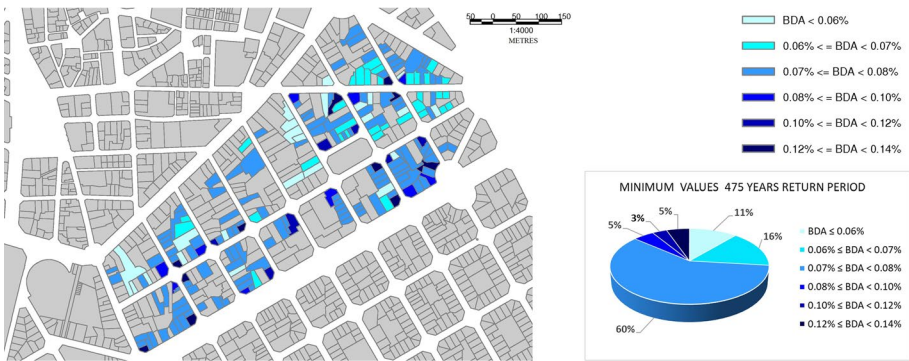**Fig. 28** Percentages of built damaged area for each scenario

Fig. 29 Built damaged area. 475 years return period minimum values (in %). Façades 480 mm thick

Fig. 30 Built damaged area. 475 years return period maximum values (in %). Façades 480 mm thick
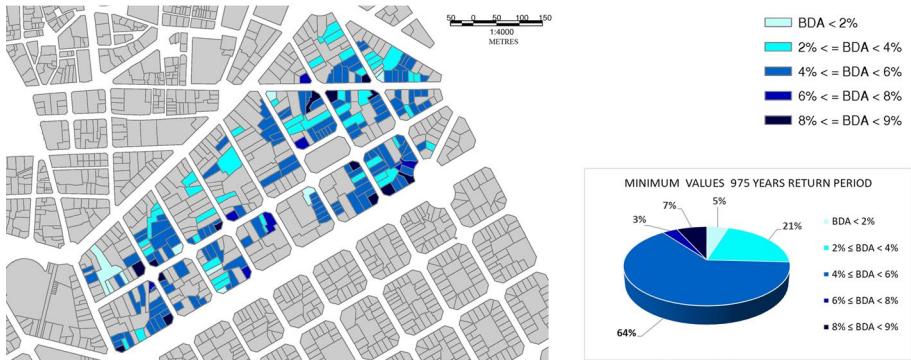
Fig. 31 Built damaged area. 975 years return period minimum values (in %). Façades 480 mm thick

Fig. 32 Built damaged area. 975 years return period maximum values (in %). Façades 480 mm thick

5 Conclusions

In this study a detailed multiscale building inventory has been created, with the records of the masonry residential buildings in *Pla del Remei* built before the end of the Spanish war (1939) and saved from demolition, integrating urban, architectural, geometrical, structural characteristics and heritage value of each building unit.

A thorough analysis of this database has been carried out to identify criteria for grouping them in order to select a reduced sample of buildings to conduct the seismic capacity and fragility assessment. With this aim, specific parameters obtained from the database have been used as input data for FaMIVE for each façade.

The capacity and fragility assessment routine of FaMIVE is used in an iterative approach to correlate the collapse load factor and capacity curves to architectural and structural features with the objective of determining homogenous typologies. Due to the existence of a very rigid building regulation in force during the studied period, the building sample has demonstrated to be quite homogeneous regarding the inter-story distances and the layout and dimension of the openings. This approach has enabled to identify geometric and architectural features obtained from onsite observation, that can be used to correlate construction to seismic response.

As a result, 14 representative typologies have been identified on the basis of the number of stories, position in the block and number of openings. This features can easily be identified by nonspecialist and using open access geographic data sources as Google street map.

Considering that the urban planning regulations in force at that time (end of the nineteenth century and beginning of the 20th) were quite similar in several Spanish cities undertaking a process of expansion of the mediaeval centres following the hygienist theories of the time, it is possible to assume that the urban characteristics (aggregation of buildings in blocks with central court and buildings in chamfers) technical data on the geometry (thickness of the load-bearing walls, dimensions and layout of the openings, inter-storey height, dimensions of the piers, balconies and parapets…) and the structural characteristics (type of masonry, mortar, horizontal structure and roof typology) determined in this study can be extrapolated to other expansion areas in Spain.

Capacity curves and fragility functions have been produced for each of the identified typologies, while each building has been considered as an independent unit for risk assessment, by assigning to it the corresponding capacity curve and fragility function, as well as the data relevant to soil classification and earthquake intensity measure.

The definition of the relevant hazard scenarios and the risk analysis have been performed with the earthquake loss estimation tool SELENA, a flexible tool that allows the user to tailor the input data according to required results, and easily integrated with FaMIVE. For the first time, SELENA has been used to compute damage and losses at the building/façade level, rather than at the urban block level, allowing to analyse the spatial distribution of damage accurately and critically assess the sensitivity of the results to the variability of the input parameters.

The uncertainties have been considered following different steps throughout the study. Uncertainties about the thickness of the bearing walls and presence of tie beams have been considered analysing different construction hypothesis, being the 480 mm thick bearing walls without tie-beams the most probable building characteristics scenario. Uncertainties about the location of the earthquake rupture have been considered by running three possible ruptures along the most probable active fault. Finally, the uncertainty in the size of the earthquake was included by defining a logic tree with three possible magnitudes of the earthquakes and corresponding weight according to the targeted PGA value.

Once the probabilistic hazard scenarios have been chosen, SELENA's output, generated for each building consisted in its probability of being in one of 5 damage states, its mean damage ratio (MDR), and economic losses computed in terms of total built damaged area (BDA). It is however impossible to compare the obtained results to real damage in buildings, as the last damaging earthquake near Valencia, known as Tavernes earthquake, occurred in 1396 (Galbis Rodriguez 1932).

Considering that 81% of the buildings are listed in any of the three listing grades, a new approach for considering the economic losses taking into account the heritage value of the buildings has been proposed as a result of a market survey.

Using the logic tree results, the minimum and maximum percentage of built damaged area for both, 475 and 975 years return periods, have been mapped for the most probable building characteristics scenario, to identify which buildings are expected to be the most damaged. Figures 29, 30, 31 and 32, show that there is a clear majority of buildings (between 51 and 64% of the building stock) performing consistently as to the level of BDA. However, while the range of possible damage levels is quite constrained for the 475 return period (either minimum or maximum scenario, achieving a maximum 10% BDA, corresponding to widespread moderate damage) for the worst 975 year return period scenario as much as 57% of the buildings could experience up to 30% to 40% BDA, corresponding to structural damage or partial

collapse. At least 10% of buildings could collapse. These results shows that for these buildings the level of risk is rather different than the one that underlines codes recommendations, therefore specific strengthening and mitigation programmes should be considered at local level, and implemented through accurate studies of the peculiarities of each building units.

A major advantage of this study, in terms of repeatability of the methodology and applicability to other studies, is that all data sources and platforms, except the original projects drawings (AHMV), are open access: the cadastral data and picture of the façades (SEC), their listed status, architectural style, and structural data (P.E.P.1), the soil characteristics (GEOWEB) and images of the urban scene (Google Street View). Moreover, also FaMIVE, SELENA and gvSIG are open access software and they can be seamlessly dovetailed and used with similarly constructed databases to conduct targeted risk analysis of historic urban centres.

Declarations

Conflict of interest All authors have no conflict of interest.

Ethical approval The research had not ethical implications, hence no approval was needed.

Informed consent No informed consent is needed.

References

Ahmad N, Crowley H, Pinho R, Ali Q (2010) Displacement-based earthquake loss assessment of masonry buildings in Mansehra City, Pakistan. J Earthquake Eng 14(sup1):1–37. https://doi.org/10.1080/13632461003651794

Akkar S, Bommer JJ (2010) Empirical equations for the prediction of PGA, PGV, and spectral accelerations in Europe, the mediterranean region, and the Middle East. Seismol Res Lett 81(2):195–206. https://doi.org/10.1785/gssrl.81.2.195

Altarriba M, Guillén C, Rojo N, Martí J, Guzmán R (2001) Una propuesta de curva mensiocronológica laterica para la ciudad de Valencia. V Congreso de Arqueología Medieval Española: actas. Valladolid, 22 a 27 de marzo 1999, vol, 1, ISBN 84-9718-010-0 pp 235–254 (**in Spanish**)

Arto I, Garrido J, Gutiérrez-Carrillo ML (2020) Seismic vulnerability analysis of medieval rammed earth fortifications in southeastern Spain. Bull Earthq Eng 18:5827–5858. https://doi.org/10.1007/s10518-020-00912-1

ASCE 7-16 (2018) Minimum design loads and associated criteria for buildings and other structures, published December 12, 2018, 17th Edition

Ajuntament de València (2005) Plan Especial de protección del Ensanche de Valencia. Pla del Remei-Russafa nord. P.E.P. 1. http://www.valencia.es/ayuntamiento/urbanismo2.nsf/vTramitacionWeb/916F20EA6146C473C12577A0004403E8?OpenDocument&Categoria=MPG [Accessed Jan 2020] (**in Spanish**)

Basset-Salom L, Guardiola-Víllora A (2014) Seismic performance of masonry residential buildings in Lorca's city centre, after the 11th May 2011 earthquake. Bull Earthq Eng 12:2027–2048. https://doi.org/10.1007/s10518-013-9559-8

Benedetti D, Benzoni G, Parisi MA (1988) Seismic vulnerability and risk evaluation for old urban nuclei. Earthq Eng Struct Dynam 16:183–201

Benito Goerlich D (ed.) (1992a) La arquitectura del Eclecticismo en Valencia. Vertientes de la arquitectura valenciana entre 1875 y 1925. 2ª ed. Ayuntamiento de Valencia, Valencia (**in Spanish**)

Benito Goerlich D (1992b) Arquitectura Modernista Valenciana. Editado por Bancaixa,Valencia (**in Spanish**)

Bernardini A, Gori R, Modena C (1990) An application of coupled analytical models and experiential knowledge for seismic vulnerability analyses of masonry buildings. In: Koridze A (ed) Engineering aspects of earthquake phenomena, vol 3. Omega Scientific, Oxon, pp 161–180

Bozorgnia Y, Abrahamson NA, Al Atik L, Ancheta TD, Atkinson GM, Baker JW, Baltay A, Boore DM, Campbell KW, Chiou BS-J, Darragh RB, Day S, Donahue JJ, Graves RW, Gregor N, Hanks T, Idriss IM, Kamai R, Kishida T, Kottke AR, Mahin SA, Rezaeian S, Rowshandel B, Seyhan E, Shahi S, Shantz T, Silva WJ, Spudich P, Stewart JP, Watson-Lamprey J, Wooddell KE, Youngs RR (2014) NGA-West2 research project. Earthq Spectra 30:973–987

Cardona OD, Ordaz MG, Reinoso E, Yamín-Lacouture LE, Barbat A.H. (2012) CAPRA—Comprehensive Approach to Probabilistic Risk Assessment: international initiative for risk management effectiveness. In: A: World Conference on Earthquake Engineering. 15th World Conference on Earthquake Engineering. Lisboa 2012, pp 1–10

Cauzzi C, Faccioli E (2008) Broadband (005 to 20 s) prediction of displacement response spectra based on worldwide digital records. J Seismol 12(4):453–475. https://doi.org/10.1007/s10950-008-9098-y

Carreño ML, Cardona OD, Barbat AH (2007) Urban seismic risk evaluation: a holistic approach. Nat Hazards 40:137–142

CEN (2004) EN 1998-1, Eurocode 8 Design of structures for earthquake resistance, part 1: general rules, seismic actions and rules for buildings. European Committee for Standardization, Brussels

CEN (2005) EN 1996-1-1, Eurocode 6 Design of masonry structures, part 1–1: General rules for reinforced and unreinforced masonry structures. European Committee for Standardization, Brussels

CEN (2006) EN 1996-1-3, Eurocode 6 Design of masonry structures, part 3: Simplified calculation methods for unreinforced masonry structures. European Committee for Standardization, Brussels

Colegio Oficial de Arquitectos de Valencia- COAV (1984) El Ensanche de la ciudad de Valencia de 1884. Edited Colegio Oficial de Arquitectos de Valencia. Valencia 1984. ISBN 84-505-0877-0. (**in Spanish**)

Colomer V, García Soria JJ (1984) La arquitectura de la calle: la calle de Cirilo Amorós. El Ensanche de la ciudad de Valencia de 1884. Edited Colegio Oficial de Arquitectos de Valencia. Valencia 1984. pp 121–136. ISBN 84-505-0877-0. (**in Spanish**)

D'ayala DF (2005) Force and displacement based vulnerability assessment for traditional buildings. Bull Earthq Eng 3:235–265. https://doi.org/10.1007/s10518-005-1239-x

D'Ayala DF, Speranza E (2003) Definition of collapse mechanisms and seismic vulnerability of historic masonry buildings. Earthq Spectra 19(3):479–509

D'Ayala DF, Paganoni S (2011) Assessment and analysis of damage in L'Aquila historic city centre after 6th April 2009. Bull Earthq Eng 9:81–104. https://doi.org/10.1007/s10518-010-9224-4

D'Ayala D (2013) Assessing the seismic vulnerability of masonry buildings. Handbook of seismic risk analysis and management of civil infrastructure systems. Woodhead publishing, Sawston, pp 334–365

D'Ayala, D., Meslem, A., Vamvatsikos, D., Porter, K., Rossetto, T., Silva, V. (2015) GEM. Guidelines for Analytical Vulnerability Assessment of Low/Mid-Rise Buildings, Vulnerability Global Component Project https://doi.org/10.13117/GEM.VULN-MOD.TR2014.12

Diodato M, Macchioni N, Brunetti M, Pizzo B, Nocetti M, Burato P, Sozzi L, Pecoraro E, Vegas López-Manzanares F, Mileto C (2015) Understanding Spanish timber jack arch floors: examples of assessment and conservation issues. Int J Archit Herit 9(6):641–654. https://doi.org/10.1080/15583058.2015.1041193

Dolsek M, Fajfar P (2004) Simplified non-linear seismic analysis of infilled reinforced concrete frames. Earthq Eng Struct Dyn 34(1):49–66

Donà M, Carpanese P, Follador V et al (2021) Mechanics-based fragility curves for Italian residential URM buildings. Bull Earthq Eng 19:3099–3127. https://doi.org/10.1007/s10518-020-00928-7

Erdik M, Durukal E (2006) Earthquake Scenarios for the city of Istanbul as a basis for preventive measures of protection. In: Proceedings of the International Forum on Earthquake Prognostics, Preventive Measures of Protection and Disaster Preparedness, March 22–24, 2006 Berlin

Erduran E, Lang DH, Lindholm C, Toma-Danila D, Balan SF, Ionescu V, Aldea A, Vacareanu R, Neagu C (2012) Real-Time earthquake damage assessment in the Romanian–Bulgarian border region. In: Proceedings of the 15 WCEE, Lisboa, 2012, p 10

Fajfar P (1999) Capacity spectrum method based on inelastic demand spectra. Earthq Eng Struct Dyn 28:979–993. https://doi.org/10.1002/(SICI)1096-9845(199909)28:9%3C979::AID-EQE850%3E3.0.CO;2-1

Fajfar P (2000) A nonlinear analysis method for performance-based seismic design. Earthq Spectra 16(3):573–592. https://doi.org/10.1193/1.1586124

Fajfar P, Dolšek M (2012) A practice-oriented estimation of the failure probability of building structures. Earthq Eng Struct Dyn 41:531–547. https://doi.org/10.1002/eqe.1143

Federal Emergency Management Agency FEMA (2003) HAZUS-MH. Multi-hazard Loss Estimation Methodology, Technical manual., Washington DC, USA

Federal Emergency Management Agency FEMA (2009). Quantification of Building Seismic Performance Factors, FEMA P-695, prepared by Applied Technology Council for the Federal Emergency Management Agency, Washington, DC

Federal Emergency Management Agency FEMA (2020). Hazus Earthquake Model, Technical Manual. Hazus 4.2 SP3. Washington DC, USA

Ferreira TM, Rui M, Romeu V (2017) Seismic vulnerability assessment of the old city centre of Horta, Azores: calibration and application of a seismic vulnerability index method. Bull Earthq Eng 15(7):2879–2899. https://doi.org/10.1007/s10518-016-0071-9

Feriche M, Vidal F, García R, Navarro M, Vidal MD, Montilla P, Piñero L (2009) Earthquake Damage Scenarios in Vélez- Málaga urban area(Southern Spain) applicable to Local Emergency Planning. In: Proceedings of the 8th international Workshop on Seismic Microzoning and Risk Reduction 15–18 March 2009. Almería (Spain)

Feriche M, Vidal F, Alguacil G, Navarro M, Aranda (2012) Vulnerabilidad y daño en el terremoto de Lorca de 2011, 7ª Asamblea Hispanoportuguesa de Geodesia y Geofísica, San Sebastián, España, 25–28 junio 2012 (**in Spanish**)

Fundación Instituto Valenciano de la Edificación (FIVE), Institut Cartogràfic Valencià (ICV) Geoweb tool. https://gvacartografic.wordpress.com/2012/03/29/geoweb-sistema-colaborativo-de-planificacion-de-estudios-geotecnicos/. Accessed from http://www.five.es:8080/geoweb/, (**in Spanish**)

Fran Bretones JM (1990) Técnicas de rehabilitación. Soluciones específicas a las lesiones del Ensanche de Valencia de 1887. Phd Thesis. Departamento de Construcciones Arquitectónicas. Universidad Politécnica de Valencia. Sept.1990. Depositada en la Biblioteca de la UPV. Signatura: B 7-2/02200. (**in Spanish**)

Galbis Rodriguez J (1932). Catálogo sísmico de la zona comprendida entre los meridianos 5º y 20W de Greenwich y los paralelos 45º y 20ºN. Instituto Geográfico Nacional, Madrid, Tomo I (**in Spanish**)

García-Mayordomo J, Insua-Arevalo JM, Martínez-Diaz JJ, Jiménez-Díaz A, Martín-Banda R, Martín-Alfageme S et al (2012) The quaternary active faults database of Iberia (QAFI v.2.0). J Iberian Geol 38(1):285–302. https://doi.org/10.5209/rev_JIGE.2012.v38.n1.39219

Giner-Robles JL, Silva PG, Rodriguez-Pascua MA, Pérez-López R, Alberola Romá A (2014). Efectos geológicos y arqueológicos producidos por el terremoto de Estubeny de 1748 AD (SE de España). Resúmenes de La 2a Reunión Ibérica Sobre Fallas Activas y Paleosismología, Lorca, España (2014), October, pp 149–152. https://doi.org/10.13140/2.1.2125.8243. (**in Spanish**)

gvSIG association (2009). gvSIG Desktop, the Open Source Geographic Information System. http://www.gvsig.com/en/home

Govern Valencià. Decret 57/1993 de 3 de maig del Govern Valencià per el cual es declara Bé d'interés Cultural el conjunt històric de València. (**in catalán**) https://dogv.gva.es/portal/ficha_disposicion.jsp?L=0&sig=1003%2F1993. (In **Catalan**)

Guardiola-Víllora A, Basset-Salom L (2020) Earthquake risk scenarios of the Ciutat Vella District in Valencia, Spain. Bull Earthquake Eng 18:1245–1284. https://doi.org/10.1007/s10518-019-00745-7

Grünthal G. (1998) European Macroseismic Scale 1998. In: Cahiers du Centre Européen de Géodynamique et de Séismologie, Luxembourg

Heath D, Wald DJ, Worden CB, Thompson EM, Scmocyk G (2020) A global hybrid VS30 map with a topographic-slope-based default and regional map insets. Earthq Spectra 36(3):1570–1584

Idealista is a Spanish company founded that offers, among others, real estate portal services via the Internet. https://www.idealista.com/maps/valencia-valencia/

IGN (2017) Actualización de Mapas de Peligrosidad Sísmica de España 2012. Editorial Centro Nacional de Información Geográfica (CNIG) DOI: https://doi.org/10.7419/162.05.217 https://www.ign.es/web/ign/portal/libros-digitales/peligrosidad-sismica2012?filtro=GEO&orden

Irizarry J, Lantada N, Pujades LG, Barbat AH, Goula X, Susagna T, Roca A (2011) Ground-shaking scenarios and urban risk evaluation of Barcelona using the Risk-UE capacity spectrum based method. Bull Earthq Eng 9:441–466. https://doi.org/10.1007/s10518-010-9222-6

Irizarry J, Macau A, Figueras S, Goula X, Lantada N, Vendrell S, Pujades LG, Blázquez A (2012) Seismic risk assessment for the city of Girona, Spain. 15th World Conference on Earthquake Engineering, *Lisbon*, Portugal, September 24–28, *2012*.

Kharazian A, Molina S, Galiana-Merino JJ, Agea-Medina N (2021) Risk-targeted hazard maps for Spain. Bull Earthq Eng 19:5369–5389. https://doi.org/10.1007/s10518-021-01189-8

Lagomarsino S, Giovinazzi S (2006) Macroseismic and Mechanical Models for the Vulnerability assessment of current buildings. Bull Earthq Eng 4(4):415–443

Lang DH, Molina-Palacios S, Lindholm CD (2008) Towards near-real-time damage estimation using a CSM-based tool for seismic risk assessment. J Earthq Eng 12(sup2):199–210. https://doi.org/10.1080/13632460802014055

Lang DH, Molina-Palacios S, Lindholm CD, Balan S (2012) Deterministic earthquake damage and loss assessment for the city of Bucharest, Romania. J Seismol 16(1):67–88

Lantada N, Irizarry J, Barbat AH, Goula X, Roca A, Susagna T et al (2010) Seismic hazard and risk scenarios for Barcelona, Spain, using the Risk-UE vulnerability index method. Bull Earthq Eng 8(2010):201–229. https://doi.org/10.1007/s10518-009-9148-z

Lantada N, Pujades LG, Barbat AH (2018) Earthquake risk scenarios in urban areas: a review with applications to the Ciutat Vella District in Barcelona, Spain. Int J Architect Herit 12(7–8):1112–1130. https://doi.org/10.1080/15583058.2018.1503367

Ley 16/1985 del Patrimonio Histórico Español Ley 16/1895 BOE-A-1985.12534. Texto consolidado. Última modificación 12 de Octubre 2021. https://www.boe.es/buscar/pdf/1985/BOE-A-1985-12534-consolidado.pdf [Accesed December 2021] (**in Spanish**)

Liu Y, Li Z, Wei B, Li X, Fu B (2019) Seismic vulnerability assessment at urban scale using data mining and GIScience technology: application to Urumqi (China). Geomat Nat Haz Risk 10(1):958–985. https://doi.org/10.1080/19475705.2018.1524400

Llopis Alonso A, Perdigón Fernández, L.A (2016) Cartografía histórica de la ciudad de Valencia (1608–1944) Editorial Universitat Politècnica de València. http://hdl.handle.net/10251/64985 (in **Spanish**)

Luco N (2006) Risk-targeted approach to selecting return periods for design maps. In: Proceedings of the 3rd ATC35/USGS National Earthquake Ground-Motion Mapping Workshop, Applied Technology Council, Redwood City, CA

Maheri MR, Pourfallah S, Azarm R (2012) Seismic retrofitting methods for the jack arch masonry slabs. Eng Struct 36:49–60. https://doi.org/10.1016/j.engstruct.2011.11.018

Martin-Rojas I, Sánchez-Alzola A, Medina-Cascales I, Borque MJ, Alfaro P, Gil AJ, Soler-Llorens JL, de Lacy MC, Andreu JM, Aviles M (2020) Surface deformation deduced from CGPS data in the eastern Betic External Zones (SE Spain). Implications on SHA, EGU General Assembly 2020, Online, 4–8 May 2020, EGU2020-17094, https://doi.org/10.5194/egusphere-egu2020-17094, 2020. https://doi.org/10.5194/egusphere-egu2020-17094.

Martínez-Cuevas S, Gaspar-Escribano JM (2016) Reassessment of intensity estimates from vulnerability and damage distributions: the 2011 Lorca earthquake. Bull Earthq Eng 14:2679–2703. https://doi.org/10.1007/s10518-016-9913-8

Martínez Solares JM, Mezcua J (2002) Catálogo Sísmico de la Península Ibérica (880 a.C. - 1900). Monografías IGN. 18. IGN. Madrid. Spain. 253 pp. (**in Spanish**)

Miján Monge R, Zalbidea Muñoz MA, Serra Lluch J (2011–2012) Revestimientos continuos tradicionales en el primer ensanche de la ciudad de Valencia. Arché. ISSN-e 2445–1150, ISSN 1887–3960, nº 6–7. págs. 293–302. http://hdl.handle.net/10251/34069 (**in Spanish**)

Ministerio de Educación, Cultura y Deporte -MECD (2015). Plan Nacional de Emergencias y Gestión de Riesgos en Patrimonio Cultural. English version available in "https://www.culturaydeporte.gob.es/planes-nacionales/dam/jcr:e57714b1-7a59-4e90-99d4-afb1f4285191/13-emergencias-y-gestion-de-riesgos-eng.pdf [Accesed December 2019]

Ministerio de Fomento (2002) Real Decreto 997/2002, de 27 de septiembre de 2002, por el que se aprueba la NCSE-02 Norma de Construcción Sismorresistente: parte General y de Edificación. Boletín Oficial del Estado, no 244: 35898–35967, España. https://cvp.mitma.gob.es/downloadcustom/sample/473 (**in Spanish**)

Ministerio de la Vivienda (1963) Norma MV 101-1962 de Acciones en la Edificación. BOE Numero 5. Del 9 de febrero de1963. (**in Spanish**)

MIT (2008) NTC 2008: Norme Tecniche per le Costruzioni. D.M. 14 Gennaio 2008 (D.M. 14/1/08) (**in Italian**)

MIT (2018) NTC 2018: D.M. del Ministero delle Infrastrutture e dei trasporti del 17/01/2018. Aggiornamento delle Norme Tecniche per le Costruzioni (**in Italian**)

Molina S, Lindholm CD (2005) A logic tree extension of the capacity spectrum method developed to estimate seismic risk in Oslo, Norway. J Earthq Eng 9(6):877–897

Molina S, Lang DH, Lindholm CD (2010) SELENA—an open-source tool for seismic risk and loss assessment using a logic tree computation procedure. Comput Geosci 36(3):257–269. https://doi.org/10.1016/j.cageo.2009.07.006

Molina S, Navarro M, Martínez-Pagan P, Pérez-Cuevas J, Vidal F, Navarro D, Agea-Medina N (2018) Potential damage and losses in a repeat of the 1910 Adra (Southern Spain) earthquake. Nat Hazards 92:1547–1571. https://doi.org/10.1007/s11069-018-3263-6

Molina, S., Martínez-Cuevas, S., Maeso, A. et al. (2020) Seismic losses scenario for the municipality of Murcia. 17Th World Conference on Earthquake Engineering, 17WCEE. Paper Nº C000500. Sendai, Japan–September 13th to 18th 2020

NRC 2015 National Building Code of Canada (NBC 2015) published by the National Research Council of Canada (NRC)

Novelli VI, D'Ayala D, Makhloufi N, Benouar D, Zekagh A (2015) A procedure for the identification of the seismic vulnerability at territorial scale. Application to the Casbah of Algiers. Bull Earthq Eng 13:177–202. https://doi.org/10.1007/s10518-014-9666-1

Pagani M, Monelli D, Weatherill G, Danciu L, Crowley H, Silva V, Henshaw P, Butler L, Nastasi M, Panzeri L, Simionato M, Vigano D (2014) OpenQuake engine: an open hazard (and risk) software for the global earthquake model. Seismol Res Lett 85(3):692–702

Pagani M, García-Pelaez J, Gee R, Johnson K, Poggi V, Silva V, Simionato M, Styron R, Viganò D, Danciu L, Monelli D, Weatherill G (2020) The 2018 version of the Global Earthquake Model: Hazard component. Earthq Spectra 36(1):226–251. https://doi.org/10.1177/8755293020931866

Perea H (2006) Falles actives i perillositat sísmica al marge nord-occidental del solc de València, PhD Thesis Universitat de Barcelona, Barcelona, p 382 (**in Catalan**)

Perea H, Masana E, Santanach P (2012) An active zone characterized by slow normal faults, the northwestern margin of the València trough (NE Iberia): a review. J Iber Geol 38(1):31–52. https://doi.org/10.5209/rev_JIGE.2012.v38.n1.39204

Putrino V, D'Ayala D (2019) Effectiveness of seismic strengthening to repeated earthquakes in historic urban contexts: Norcia 2016 Disaster Prev. Manag Int J 29:47–64. https://doi.org/10.1108/DPM-07-2018-0230

Revista Obras Públicas-ROP (1903a) Muros de ladrillo. Ensayos de resistencia. Experiencias realizadas en Londres por el Royal Institute of British Architects. Tomo I. 38:116. Retrieved from https://quickclick.es/rop/pdf/publico/1903/1903_tomoI_38.pdf (**in Spanish**)

Revista Obras Públicas-ROP (1903b) Muros de ladrillo. Ensayos de resistencia. Experiencias realizadas en Londres por el Royal Institute of British Architects. Tomo I. 40:119. Retrieved from https://quickclick.es/rop/pdf/publico/1903/1903_tomoI_40.pdf (**in Spanish**)

Ruiz-Pinilla JG, Adam JM, Pérez-Cárcel R, Yuste J, Moragues JJ (2016) Learning from RC building structures damaged by the earthquake in Lorca, Spain, in 2011. Eng Fail Anal 68:76–86. https://doi.org/10.1016/j.engfailanal.2016.05.013

Scherbaum F, Schmedes J, Cotton F (2004) On the conversion of source-to-site distance measures for extended earthquake source models. Bull Seismol Soc Am 94(3):1053–1069

Sedan O, Negulescu C, Terrier M, Roulle A, Winter T, Bertil D (2013) Armagedom. A tool for seismic risk assessment illustrated with applications. J Earthq Eng 17(2):253–281. https://doi.org/10.1080/13632469.2012.726604

Sede Electrónica del Catastro (SEC) (2022) Access to the Cadastral Database. https://www1.sedecatastro.gob.es. Last accessed Dec 2020–Jun 2022

Shabani A, Kioumarsi M, Zucconi M (2021) State of the art of simplified analytical methods for seismic vulnerability assessment of unreinforced masonry buildings. Eng Struct 239:112280. https://doi.org/10.1016/j.engstruct.2021.112280

Taberner Pastor F (1984) El ensanche de Valencia: trazado y realidad urbana. El Ensanche de la ciudad de Valencia de 1884. Edited: Colegio Oficial de Arquitectos de Valencia. Valencia 1984. pp 121–136. ISBN 84-505-0877-0 (**in Spanish**)

Taberner Pastor F, Broseta Palanca MT (2014) Arquitectura y desarrollo urbano. Notas sobre el ensanche de Valencia de 1884. Archivo de Arte Valenciano. XCV:181–200. (**in Spanish**) https://realacademiasan

carlos.com/download/105/2014-xcv/1XkAypzdbn5LFrI3ZTi_6qI5FNdix4Tme/Francisco%20Taberner%20Pastor%20y%20M%C2%AATeresa%20Broseta%20Palanca.pdf

Torelli G, D'Ayala D, Betti M, Bartoli G (2020) Analytical and numerical seismic assessment of heritage masonry towers. Bull Earthq Eng 18(3):969–1008. https://doi.org/10.1007/s10518-019-00732-y

Vettore M, Donà M, Carpanese P, Follador V, da Porto F, Valluzzi MR (2020) A multilevel procedure at urban scale to assess the vulnerability and the exposure of residential masonry buildings: the case study of Pordenone, Northeast Italy. Heritage 3:1433–1468. https://doi.org/10.3390/heritage3040080

Vidal F (1986) Sismotectónica de la Región Béticas-Mar de Alborán. Tesis Doctoral, Universidad de Granada, Granada, pp. 480. (**in Spanish**)

Authors and Affiliations

Arianna Guardiola-Víllora[1] [ORCID] **· Sergio Molina[2,3] · Dina D'Ayala[4]**

✉ Arianna Guardiola-Víllora
  aguardio@mes.upv.es

1   Departamento de Mecánica de Medios Continuos y Teoría de Estructuras, Universitat Politècnica de València, Cno de Vera s/n, 46022 Valencia, Spain

2   Instituto Multidisciplinar para el Estudio del Medio Ramón Margalef (IMEM), Universidad de Alicante (UA), San Vicent del Raspeig, Alicante, Spain

3   Departamento de Física Aplicada, Universidad de Alicante (UA), San Vicent del Raspeig, Alicante, Spain

4   Department of Civil Environmental Geomatic Engineering, University College London, London, UK